

## Article

# Lignin Depolymerization in the Presence of Base, Hydrogenation Catalysts, and Ethanol

Iuliia Romanenko<sup>1</sup>, Felix Kurz<sup>1</sup>, Robert Baumgarten<sup>1</sup>, Ivana Jevtovikj<sup>1,\*</sup> , Jean-Pierre Lindner<sup>2</sup>, Arunabha Kundu<sup>3</sup>, Alois Kindler<sup>2</sup> and Stephan Andreas Schunk<sup>2,\*</sup> 

<sup>1</sup> Hte GmbH, the High Throughput Experimentation Company, Kurpfalzring 104, 69123 Heidelberg, Germany; romanenko.iuliia@gmail.com (I.R.); felix.kurz@live.de (F.K.); robert.baumgarten@campus.tu-berlin.de (R.B.)

<sup>2</sup> BASF SE, Carl-Bosch Strasse 38, 67056 Ludwigshafen, Germany; jean-pierre-berkan.lindner@basf.com (J.-P.L.); alois.kindler@basf.com (A.K.)

<sup>3</sup> BASF Corporation, 23800 Mercantile Road, Beachwood, OH 44122, USA; arunabha.kundu@basf.com

\* Correspondence: ivana.jevtovikj@hte-company.de (I.J.); stephan.schunk@hte-company.de (S.A.S.); Tel.: +49-6221-7497-349 (I.J.); +49-6221-7497-111 (S.A.S.)

**Abstract:** Being the major renewable source of bio-aromatics, lignin possesses considerable potential for the chemical industry as raw material. Kraft lignin is a couple product of paper industry with an annual production of 55,000,000 ton/y and is considered the largest share of available lignin. Here we report a facile approach of Kraft lignin depolymerization to defined oligomeric units with yields of up to 70 wt.%. The process implies utilization of an aqueous base in combination with a metal containing catalyst and an alcohol under non-oxidative atmosphere at 300 °C. An advantage of the developed approach is the facile separation of the oligomer product that precipitates from the reaction mixture. In addition, the process proceeds without char formation; both factors make it attractive for industrialization. The suppression of the repolymerization processes that lead to char formation is possible when the combination of metal containing catalyst in the presence of an alcohol is used. It was found that the oligomer units have structural features found in phenol-acetaldehyde resins. These features result from the base catalyzed condensation of lignin fragments with in situ formed aldehydes. Catalytic dehydrogenation of the alcohol provides the latter. This reaction pathway is confirmed by the presence condensation products of Guerbet type reactions.

**Keywords:** Kraft lignin; base catalyzed depolymerization; heterogeneous catalysis



**Citation:** Romanenko, I.; Kurz, F.; Baumgarten, R.; Jevtovikj, I.; Lindner, J.-P.; Kundu, A.; Kindler, A.; Schunk, S.A. Lignin Depolymerization in the Presence of Base, Hydrogenation Catalysts, and Ethanol. *Catalysts* **2022**, *12*, 158. <https://doi.org/10.3390/catal12020158>

Academic Editors: Juan J. Bravo-Suarez, Qiying Liu, Michael Renz, Anna Maria Raspolli Galletti, Rafael Luque and Gartzen Lopez

Received: 22 December 2021

Accepted: 22 January 2022

Published: 27 January 2022

**Publisher's Note:** MDPI stays neutral with regard to jurisdictional claims in published maps and institutional affiliations.



**Copyright:** © 2022 by the authors. Licensee MDPI, Basel, Switzerland. This article is an open access article distributed under the terms and conditions of the Creative Commons Attribution (CC BY) license (<https://creativecommons.org/licenses/by/4.0/>).

## 1. Introduction

In the context of increasing greenhouse gas emissions, the search for renewable resources that can be integrated into petrochemical value chains becomes more and more pressing [1]. One attractive raw material pool is the valorization of lignocellulosic biomass. Lignocellulosic biomass consists of three main components: cellulose (40–60%), hemicellulose (10–40%), and lignin (15–30%). In the concept of a sustainable development plan the potential of valorization of all three components should be evaluated in light of petrochemical products of value with the minimum energy demand and associated waste generation [2,3]. So far, most of the developed processes are focused on valorization of the sugar containing bio-polymers of lignocellulosic biomass. The classical example is Kraft process that is used in the paper industry to produce pure cellulose from lignocellulosic biomass. In this case lignin is obtained as a side product with the global production of 55,000,000 ton/y [4]. Currently, Kraft lignin is thermally valorized to produce steam and electricity for running a paper mill, and the base contained in Kraft lignin is recycled after the incineration. Due to significant efforts to debottleneck the paper industry and to co-produce sustainable raw materials efficiently, together with elaboration of new technologies like the LignoBoost® process [5], an increasing amount of Kraft lignin has become available for the market.

While Kraft lignin found an application as a cheap fuel, its full potential remains underutilized. Indeed, lignin is up to this point the only available renewable source for bioaromatics. Its structure could be described as an interconnected network of phenolic monomers, mostly represented by p-coumaryl alcohol, coniferyl alcohol, and sinapryl alcohol, which is linked together by ether and C-C linkages [6–9]. From this point of view, lignin valorization opens new perspectives in the field of composite materials, petrochemicals, and in the recent years also fine chemicals like aromatic amines [10–12].

Therefore, several approach including base-catalyzed [13,14], acid-catalyzed [15], reductive [2,16], oxidative [17,18], and thermal [19–21] methods have been applied for lignin valorization [22,23]. However, the development of an effective lignin valorization process faces several obstacles. The first one is related to the fact that the structure of lignin varies significantly depending on the botanic origin of the biomass, as well as the details of the aftertreatment process. Thus, Kraft lignin has a higher amount of recalcitrant bonds (C-C linkages) compared to native lignin which contains mostly ether linkages, among which the  $\beta$ -O-4 moieties is the most abundant (Figure 1). In addition, Kraft lignin has high content of sulfur 2–3% that makes the search of effective sulfur-resistant depolymerization catalysts challenging [23,24]. Another obstacle is the tendency of obtained phenolic monomers to repolymerize; in most cases this repolymerization leads to char formation and results in coking of the catalyst or even in reactor clogging [25,26]. Apparently repolymerization processes are enhanced at higher reaction temperatures. On the other side, high reaction temperatures are required for efficient lignin depolymerization.

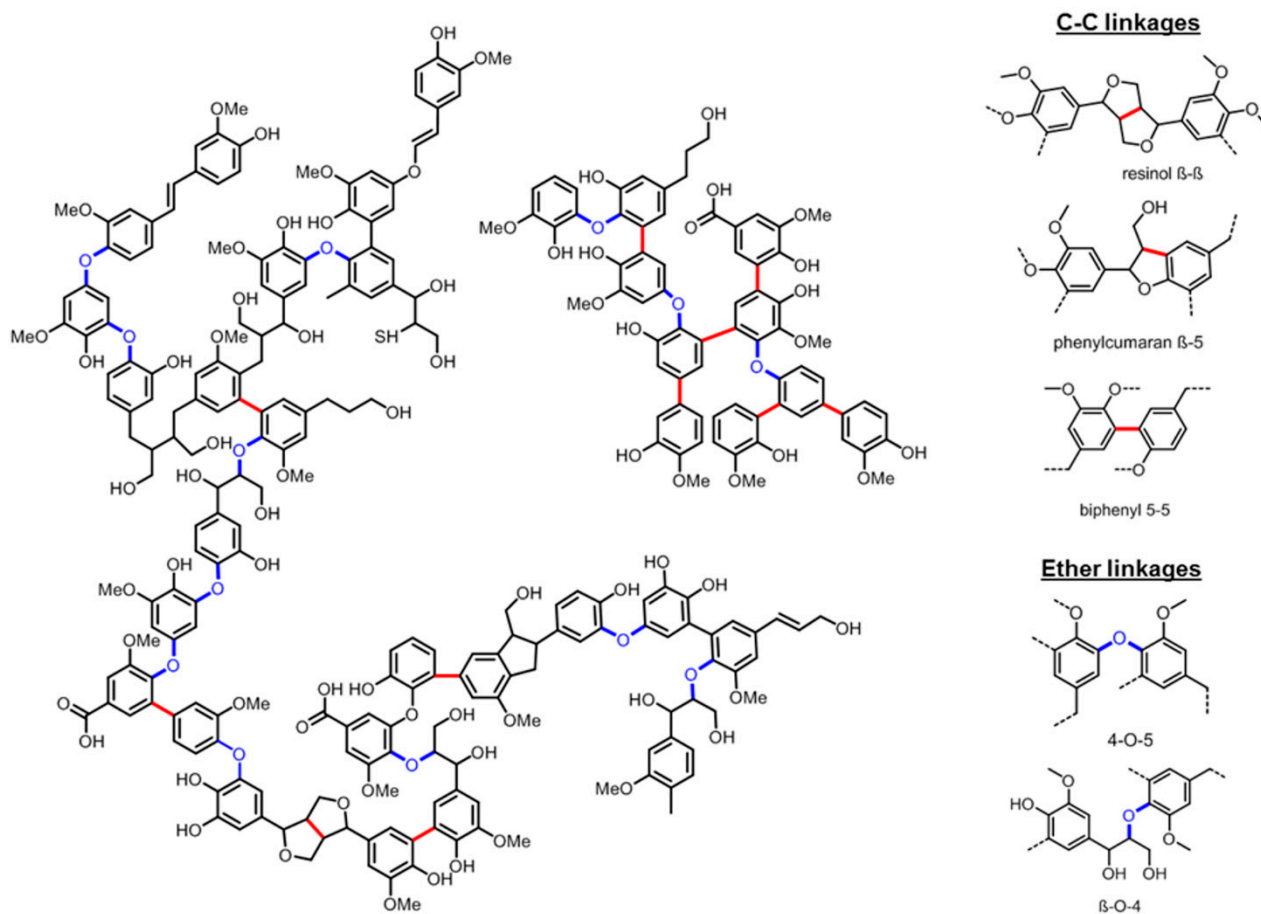


**Figure 1.** Chemical structure of Kraft lignin.

Nevertheless, reductive lignin depolymerization, in the presence of hydrogen and a hydrogenation catalyst, was found to be the most successful, among other approaches, as it resulted in a lower amount of char formation. The role of the heterogeneous cat-

alyst is reported to assist in the reduction of alkenyl, carbonyl, and terminal alcohol groups that tend to condensate. Typically, heterogeneous catalysts like Pd/C [27,28], Pt/C [29], Pt/Al<sub>2</sub>O<sub>3</sub> [28], Ru/C [28–33], Ni/C, and Raney Nickel [34] are used for reductive lignin depolymerization.

Depolymerization at significantly suppressed repolymerization tendency was also found to be possible by using alcohols as a solvent in combination with hydrogenation catalysts. Ford and colleagues reported successful lignin depolymerization with formation of negligible amount of char by utilizing Cu-doped porous metal oxide catalyst (Cu-PMO) in supercritical methanol. The reaction proceeded at 300–320 °C for 2–12 h and resulted in lignin monomers mostly represented by cyclohexyl derivatives suggesting that methanol is not a neutral solvent and acts as a hydrogen source [35–37]. Later Huang et al. studied the effect of supercritical ethanol on lignin depolymerization with Cu-doped MgAl mixed oxide (CuMgAlO<sub>x</sub>) as a catalyst at 300 °C for 4–8 h. In this case the high yield of deoxygenated monoaromatics was obtained without char formation. Authors reported the low ring-hydrogenation activity of catalyst. The detailed NMR investigation together with GC-MS analysis reveals that ethanol acts as a capping agent resulting in O-alkylation of phenolic hydroxyl and C-alkylation of aromatic rings. The alkylation suppresses the repolymerization of phenolic monomers that leads to char formation. Comparison of ethanol with methanol shows that using ethanol as solvent results in higher monoaromatics yield, probably due to the ability of ethanol to act as a scavenger of formaldehyde derived from lignin depolymerization [38,39]. The application of supercritical tert-butanol as a solvent was investigated by Choi et al. The lignin depolymerization was performed using a combination of supercritical tert-butanol with supported metal catalyst like Pt/C, Pd/C, Ru/C, and Ni/C at 350 °C for 40 min. Addition of a catalyst helps to decrease the total amount of char, however the full suppression of the repolymerization process was not possible [40]. On the contrary performing lignin depolymerization under same conditions but using ethanol instead of tert-butanol resulted in high yields of monoaromatics and almost no char formation. Thus the nature of the alcohol seems to play a crucial role in suppression of the repolymerization process [41]. The utilization of alcohol as an additive and reagent in acid/base-catalyzed lignin depolymerization has also been reported [42–54]. Watanabe and coworkers showed that the acid-catalyzed degradation of lignin in a hydrophobic solvent like toluene, containing a small amount of methanol under mild temperatures 140–170 °C, helps to suppress char formation. Obtained in this case were monoaromatics existing in the form of dimethyl acetal derivatives due to reaction of in situ formed enol ether with alcohol [55].

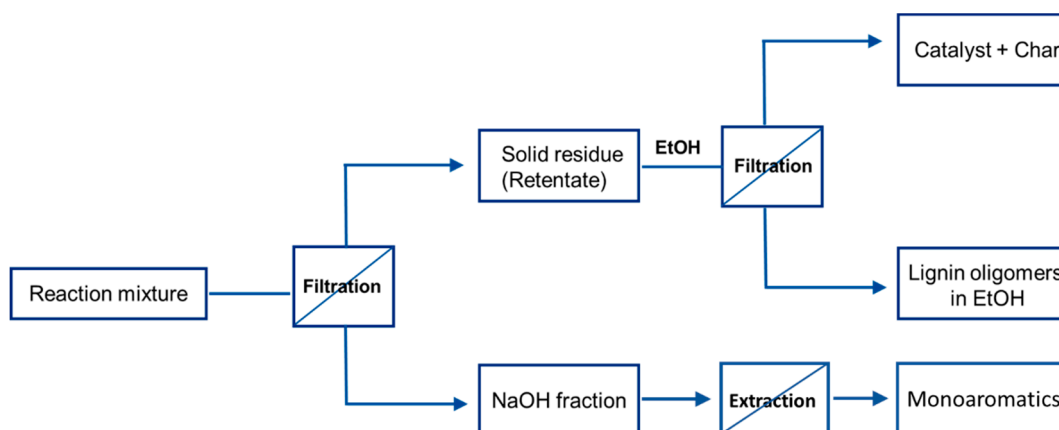
In this work, we combined the base catalyzed depolymerization approach, with the reductive treatment in presence of alcohols and metal catalysts and obtained high yields of defined oligomeric products with low molar mass and polydispersity index. The use of a hydrogenation/dehydrogenation catalyst in the presence of an alcohol was found to minimize char formation, while an inorganic base serves as depolymerization catalyst.

## 2. Results and Discussions

### 2.1. Kraft Lignin Depolymerization in Alkaline Media in the Presence of Ru/C Catalyst and Ethanol

The initial attempt to depolymerize lignin in the presence of both hydrogenation/dehydrogenation catalyst and base was done by using Ru/C catalyst. Ru/C is known to be an effective hydrogenation/dehydrogenation catalyst, as well as the cheapest one among all PGM metals. The depolymerization performed at 300 °C under 30 bar (120 barg) of H<sub>2</sub> in the presence of 10 wt.% ethanol, and 1 M NaOH as it was shown that presence of alcohol helps to overcome undesirable char formation [32,33]. After 6 h of reaction the formation of tar-like precipitate in the yield of 51 wt.% was detected. The obtained precipitate could be easily isolated by means of filtration (Scheme 1). Surprisingly, the retentate was found to be completely soluble in ethanol, DMSO, THF, and acetone and insoluble in water and toluene. This allowed easy separation of the retentate from the insoluble Ru/C catalyst and char by means of dissolution in ethanol. The weight of the insoluble residue was even with

the weight of Ru/C catalyst, suggesting that no apparent char formation took place under applied conditions. Interestingly, performing the same reaction without Ru/C catalyst results in massive char formation.



**Scheme 1.** Work-up procedure for separation of lignin oligomers and catalyst from reaction media.

Obtained ethanol soluble retentate, filtrate, and starting material were analyzed by gel permeation chromatography (Figure 2). The starting Kraft lignin has an average molar mass of 1400 g/mol and polydispersity index of 7.3. Both retentate and filtrate fraction show considerable mass decrease down to 600 g/mol in comparison with the starting Kraft lignin, as could be seen by shift of the maximum of the molecular weight distribution curve of lignin towards lower molar masses. In addition, both fractions have a moderate polydispersity index in the range of 2.2–2.4.

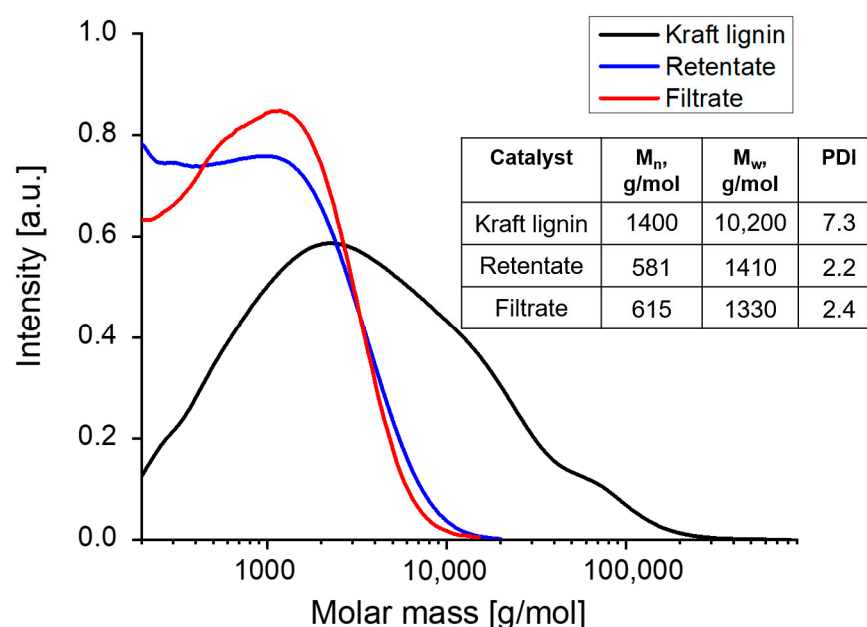


**Figure 2.** GPC chromatograms of starting Kraft lignin, retentate, and filtrate fractions of product obtained by depolymerization of Kraft lignin (10 wt.%) at 300 °C for 6 h in the presence of Ru/C catalyst (2.6 wt.%), ethanol (10 wt.%), 30 bar (120 barg) of H<sub>2</sub>, and 1 M NaOH (80 wt.%). DMSO + LiBr was used as an eluent.

The success of depolymerization was also confirmed by DSC measurements that show significant decrease of glass transition temperature from 144.3 °C for starting Kraft lignin to 21.5 °C for lignin oligomers (retentate) (Appendix A, Figure A1).

Besides a decrease of molecular weight, significant changes in the elemental composition of retentate phase in comparison with starting Kraft lignin were identified (Table 1). Indeed, retentate has significantly lower oxygen content and significantly higher carbon content. The O/C ratio of 0.17 was determined for the precipitated lignin oligomers while starting Kraft lignin has a value of 0.46. In contrast, the filtrate shows an increase in oxygen and a decrease in carbon content that results in 0.62 O/C ratio. The change in elemental composition of both fractions suggests that besides depolymerization, an additional chemical transformation took place during the applied process.

**Table 1.** Elemental composition of starting Kraft lignin and retentate.

Entry	Sample	C (wt.%)	O (wt.%)	H (wt.%)	O/C
1	Kraft lignin	64.3	29.7	6.0	0.46
2	Retentate	78.7	13.3	8.0	0.17
3	Filtrate	57.5	35.7	6.8	0.62

With the aim to identify the chemical transformation that took place during depolymerization, the precipitated lignin oligomers (retentate) were additionally characterized by FT-IR, 2D NMR.

The IR analysis clearly shows (Figure 3) that retentate contains most of the signals initially present in Kraft lignin, including the peaks of aromatics at 650–900  $\text{cm}^{-1}$  and 1600–1450  $\text{cm}^{-1}$  associated with out of plane C-H bindings and C=C in-plane vibrations correspondingly. Wang et al. suggested that increased absorption at 1568  $\text{cm}^{-1}$  is a sign of formation of highly organized aromatic residue [56]. Obtained retentate also has strong absorption at 1375  $\text{cm}^{-1}$  and in the region of 3000–3600  $\text{cm}^{-1}$  that corresponds to the C-O and O-H stretching mode of phenolic species. Interestingly, C-O stretching at 1120  $\text{cm}^{-1}$  associated with  $\beta$ -O-4 bond is absent in the spectrum of retentate, suggesting successful depolymerization. The presence of both hydroxyl groups and aromatic rings suggests that depolymerization proceeds with preservation of phenolic units. Indeed, Ru/C is known to take part in hydrogenation of aromatics, however it seems to be not the case under applied reaction conditions. In addition, strong peaks at 2869  $\text{cm}^{-1}$ , 2925  $\text{cm}^{-1}$ , and 2957  $\text{cm}^{-1}$  related to the C-H stretching of alkyl chain appear in the spectra of retentate. The remains of those peaks could also be identified in the initial Kraft lignin with the intensities close to the noise level.

The spectrum of the obtained retentate was further compared with known monolignols that were reported in the literature as possible products of lignin depolymerization: 3-Hydroxypropyl-2-methoxyphenol and 2-methoxy-4-phenol (Figures A2 and A3). The difference between both could be noticed in the region 2500–3600  $\text{cm}^{-1}$  that is attributed to the C-H stretching of propyl chain (2700–3000  $\text{cm}^{-1}$ ) and OH stretching (3550–3200  $\text{cm}^{-1}$ ). The results showed a bigger similarity of retentate to 2-methoxy-4-phenol. The bands in retentate spectrum located in the region 2500–3600  $\text{cm}^{-1}$  are almost identical to the ones found in 2-methoxy-4-phenol, suggesting that depolymerized lignin does not contain terminal OH. On the other hand, depolymerized product (retentate) contains phenolics and alkyl chain presumably propyl.

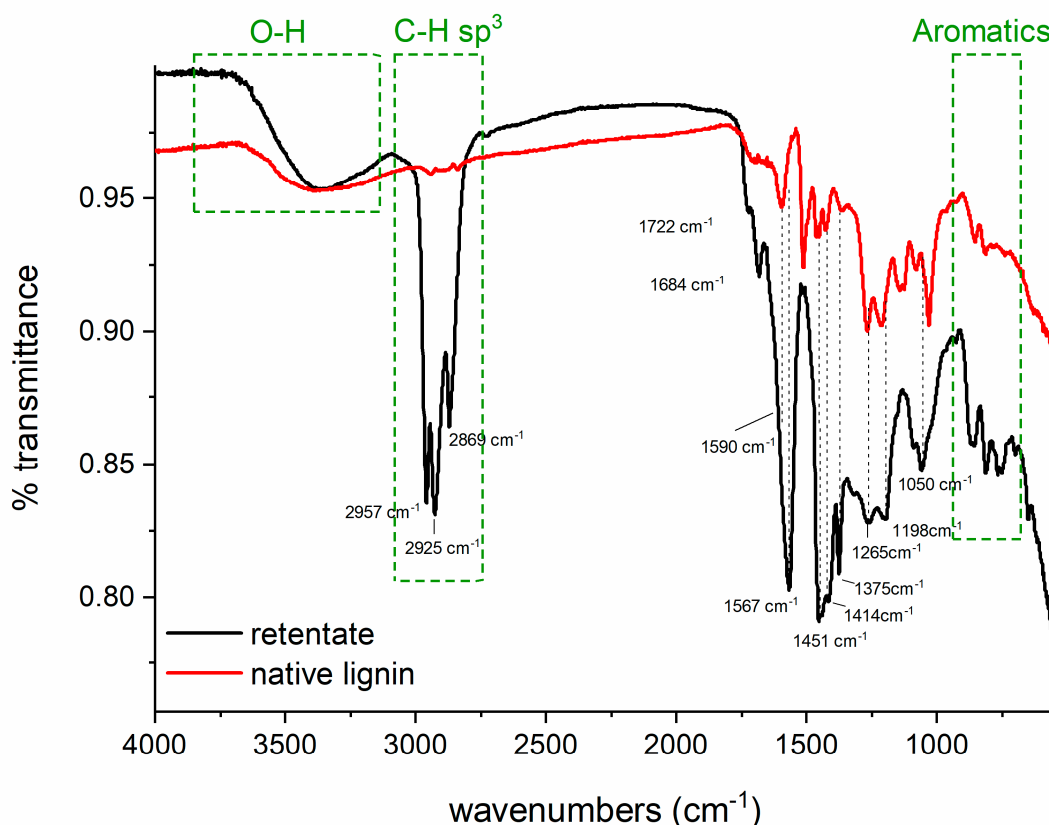


**Figure 3.** FT-IR spectrum of starting Kraft lignin and precipitated lignin oligomers (retentate).

The success of depolymerization was also confirmed by NMR spectroscopy. A 2D  $^1\text{H}$ - $^{13}\text{C}$  HSQC NMR of Kraft lignin (Figure 4, top) reveals that monomeric units are linked together in an interconnected polymer network by different linkages that are realized by formation of several structural moieties. The cross peaks at  $\delta_{\text{C}}/\delta_{\text{H}}$  60–65/3.2–3.7 ppm are attributed to the protons linked to *B* and  $\gamma$  carbons in  $\beta$ -O-4 linkage in 5-aryl ether structure (A). Other structures like resinol (C) (series of cross peaks at  $\delta_{\text{C}}/\delta_{\text{H}}$  85.03/4.63, 53.69/3.07, and 70.98/4.17 attributed to protons linked to *A*, *B*, and  $\gamma$  carbons accordingly) and phenylcumaran (B) ( $\delta_{\text{C}}/\delta_{\text{H}}$  86.72/5.48 attributed to proton at *A* position) were detected as well. The integration of protons attached to *A* carbon in each structure allowed us to calculate the relative ratio of linkages: 42% of A ( $\beta$ -O-4 linkage), 37% of C ( $\beta$ - $\beta$  linkage), and 21% of B ( $\beta$ -5 linkage). Interestingly, the precipitated product does not have any x-correlation peaks in the region of  $\delta_{\text{C}}/\delta_{\text{H}}$  50–90/3.0–4.5 ppm associated with  $\beta$ -O-4,  $\beta$ - $\beta$ , and  $\beta$ -5 linkages, previously observed in Kraft lignin (Figure 4, bottom). This strongly indicates that under the applied conditions almost quantitative cleavage of ether linkages occurs, resulting in subsequent lignin depolymerization as it is shown by GPC analysis.

The other difference in the spectra of obtained lignin oligomers versus starting Kraft lignin can be found at  $\delta_{\text{C}}/\delta_{\text{H}}$  55–56/3.5–4.5 ppm. This cross-correlation is assigned to the  $-\text{OCH}_3$  groups of the aromatic core of guaiacyl units (G). Consequently, this signal is absent in the spectrum of precipitated lignin oligomers. It was already reported that under high temperatures, and in the presence of reductive atmosphere, methoxy groups can be cleaved off. As evidence of this hypothesis, in the experiment of lignin depolymerization performed in the absence of an alcohol (250 °C, 30 bar of  $\text{H}_2$ , NaOH, 6 h), methanol was detected as a byproduct.

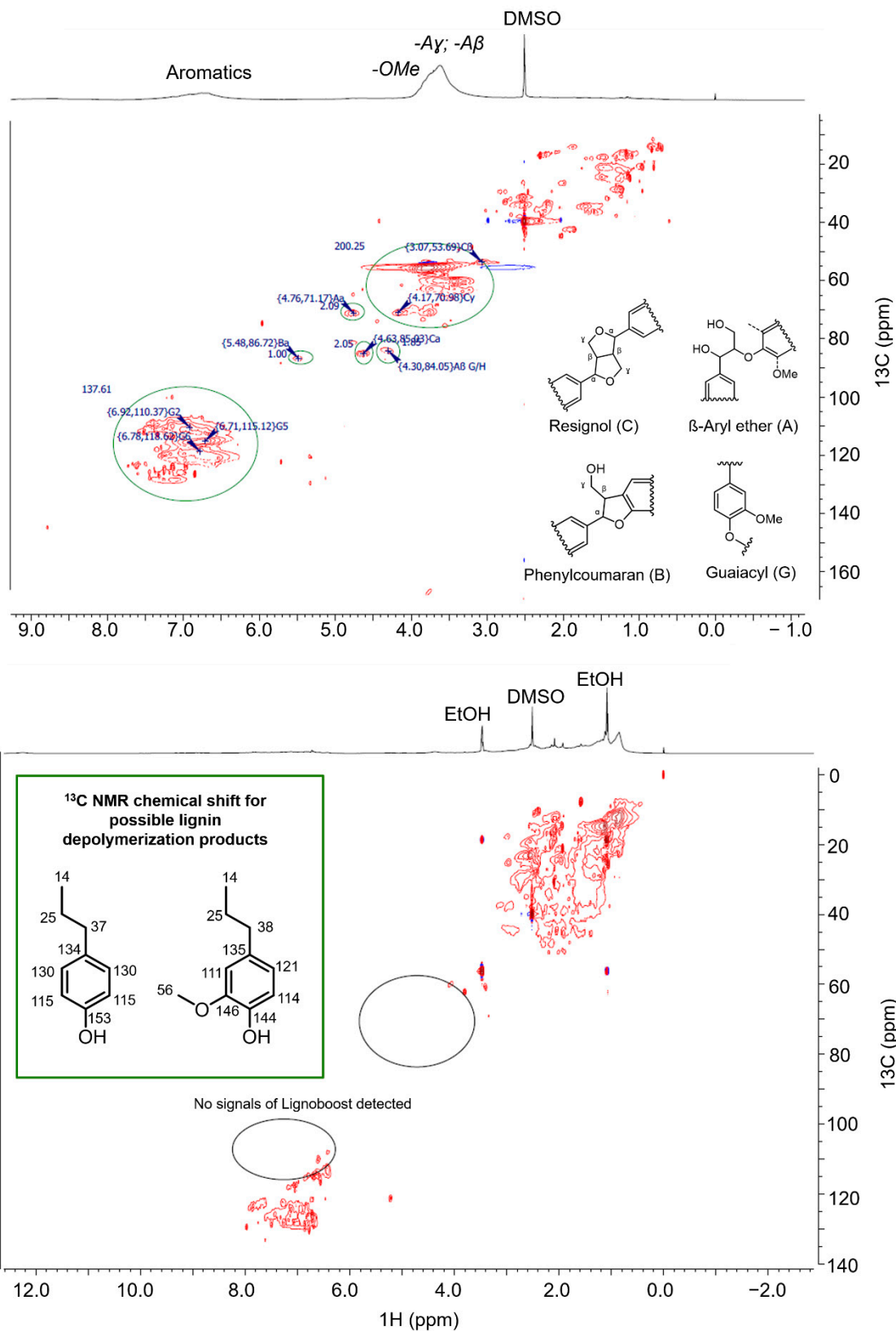


Figure 4.  $^1\text{H}$ - $^{13}\text{C}$  HSQC NMR spectrum of Kraft lignin (top) and precipitated lignin oligomers (bottom).

The cleavage of methoxy groups also provokes changes in the aromatic region in the spectrum of retentate. The starting Kraft lignin (Figure 4, top) displayed aromatic signals in the region of  $\delta C/\delta H$  105–120/6.2–7.7, which is due to the presence of electron withdrawing methoxy groups. On the contrary, the aromatic signals of the lignin oligomer are shifted to  $\delta C/\delta H$  120–130/6.8–8.0, which is caused by the absence of  $-OCH_3$  group attached to aromatic cores. Comparison of chemical shifts of the obtained lignin-oligomer and monomers resembling lignin repeating units (e.g., 4-propylphenol and 2-methoxy-4-propylphenol, Figure 4, bottom inset) revealed significant similarity. The shifts of 4-propylphenol seem to fit best to the obtained structure.

Another significant difference is the increase of aliphatic-protons in the region  $\delta C/\delta H$  10–50/0.8–3.0. The change of the aromatic to aliphatic ratio from 1:0.5 for starting Kraft lignin to 1:7 in case of retentate (determined by integration of corresponding regions in  $^1H$  NMR spectra) could not be explained just by hydrogenation of the aromatic ring structures. The scope of aliphatic signals covers the range from 0.9–3.0 ppm, which is much bigger than 1.2–1.6 ppm, where cyclohexane is usually observed. In addition, the presence of aromatics as well as an increase of aliphatics in lignin oligomer was confirmed by IR-spectroscopy, which suggests that 2-Methoxy-4-Propylphenol is a close analogue of obtained lignin oligomers. Similarity between with 2-Methoxy-4-Propylphenol and retentate could be also found in NMR spectrum, where the broad peaks at 0.9, 1.6, and 2.6 ppm fit to the methyl and methylene group of propyl chain.

A similar increase of aliphatics, as well as a decrease in aromatics protons during lignin depolymerization, have been also observed by Huang et al. in the reaction performed in supercritical alcohols, using  $CuMgAlO_x$  catalyst at 300 °C for 4 h [33]. The authors explained the observed phenomena by extensive C- and O-alkylation of depolymerized lignin monomers. In our case no signals related to O-alkylation can be observed in NMR; however, C-alkylation could not be fully excluded.

The 2D  $^1H$ - $^{13}C$  HMBC NMR also suggests that precipitated lignin oligomers have a very uniform structure (Figure 5 bottom). Indeed, the spectrum of retentate seems to be less busy in comparison with the starting Kraft lignin with a high number of cross-correlation peaks due to the complex structure of the polymer (Figure 5 top). The most pronounced correlation in the spectrum of Kraft lignin is at  $\delta C/\delta H$  150/6.5–7.5 ppm (2), which is assigned to aromatic protons in proximity to quaternary, heteroatom bound aromatic carbon (CH-C(OH)-CH). This proves the presence of phenolic groups in the polymer structure. The cross peaks  $\delta C/\delta H$  150/6.5–3.9 ppm (1) result from correlation of protons of  $-OCH_3$  group with quaternary, heteroatom bound aromatic carbon (CH-C(OH)-CH).

In the spectrum of lignin oligomers, the presence of phenolic OH could also be confirmed by cross peak at  $\delta C/\delta H$  150/6.8 ppm (1), which displays interaction of aromatic protons to aromatic, quaternary, heteroatom bound carbon. The additional cross peaks at  $\delta C/\delta H$  150/2.2 ppm and  $\delta C/\delta H$  150/2.6 ppm are attributed to correlation of the same quaternary carbon atom with  $-CH_2-$  groups of alkyl chains (2). These kinds of correlations have not been seen in the starting Kraft lignin, indicating successful lignin depolymerization and methoxy group elimination resulting in a more homogeneous structure. Additional cross peaks at  $\delta C/\delta H$  128/2.2 ppm (4) and  $\delta C/\delta H$  128/2.6 ppm (3) show correlation of alkyl protons with aromatic carbons in position 3, 4, 5. The absence of a correlation between  $-OCH_3$  group and aromatic carbons ( $\delta C/\delta H$  125–150/0.8–0.9 ppm) again confirms the elimination of methoxy groups. Like Kraft lignin, the obtained 'oligomer' product contains peaks attributed to aldehydes and acids. Interestingly, cross peaks attributed to aldehydes show different chemical shifts for both product and starting material, whereas the cross-peaks for acids and esters are overlapping. Apparently, acid and ester groups stay intact during lignin depolymerization.

The results obtained by 2D NMR are in correlation with the  $^{31}P$  NMR (Figure S2), showing significant decrease in aliphatic and aromatic OH-groups in the retentate product in comparison to the starting Kraft lignin, while the amount of acid functionalities remains intact (Table S3).

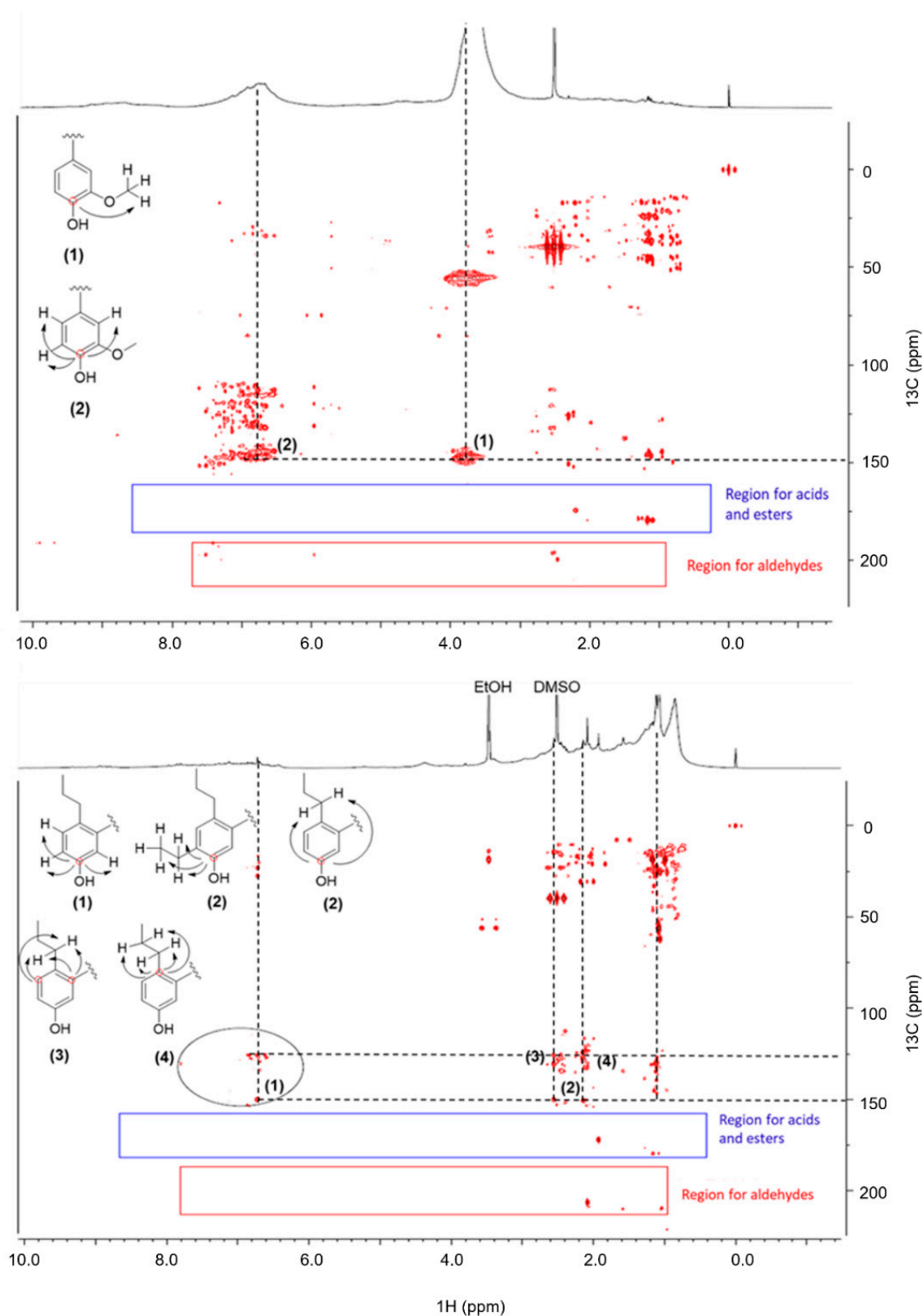


**Figure 5.**  $^1\text{H}$ - $^{13}\text{C}$  HMBC NMR spectrum of Kraft lignin (**top**) and precipitated lignin oligomers (**bottom**).

## 2.2. Catalyst Screening

With the aim to decrease the total costs of a future lignin depolymerization process different heterogeneous Cu and Ni-based catalysts were tested. The characteristics of retentates obtained by using different catalyst are summarized in Table 2. The initial

reaction performed with 0.01 wt.% Ru/C catalyst (based on metal loading) and resulted in  $49 \pm 09$  wt.% of retentate with number weighted molar mass of  $539 \pm 31$  g/mol and moderate polydispersity index of  $2.3 \pm 0.1$  (Table 2, entry 1). Performing the reaction with same catalyst loading (metal based) of commercial Raney Ni resulted in the lowest molecular weight of retentate of 385 g/mol and the smallest polydispersity index of 1.6 among all tested catalysts (Table 2, entry 2). The yield of the product was considerably lower, reaching only 34 wt.%. However, using Ni nanoparticles (NPs) as a catalyst results in comparable yield of retentate with similar characteristics previously obtained with Ru/C. Thus, Ni NPs could be considered as a cheap alternative to Ru/C.

**Table 2.** Characteristics of retentate obtained by lignin depolymerization with different catalysts. Lignin depolymerization performed with Kraft lignin (10 wt.%) at 300 °C for 6 h in the presence of catalyst (0.01–0.36 wt.%, metal based), ethanol (10 wt.%), 30 bar (120 barg) of H<sub>2</sub>, and 1M NaOH (80 wt.%). DMSO + LiBr was used as an eluent for GPC.

Entry	Catalyst	Cat. Amount, (wt.%)	M <sub>n</sub> (g mol <sup>-1</sup> )	M <sub>w</sub> (g mol <sup>-1</sup> )	PDI	Yield of Retentate (wt.%)
1	Ru/C	0.01	539 ± 31	1247 ± 116	2.1 ± 0.1	49 ± 09
2	Raney Ni	0.01	385	632	1.6	34
3	Ni NPs	0.01	519	1120	2.2	48

### 2.3. Effect of Alcohol Addition

To understand the effect of alcohol in lignin depolymerization the series of experiments with variation of alcohol amount and nature was performed (Table 3). The blank experiment without addition of ethanol did not yield oligomer formation in the form of ethanol soluble retentate (Table 3, entry 1). Instead, the mediocre amount of char was found suggesting that the presence of alcohol is highly important for both precipitation of lignin oligomers and suppressing charring. The increase of the amount of ethanol, however, does not result in better outcome. Indeed, the obtained retentate was more soluble in the reaction medium due to the presence of ethanol. Thus, for improved precipitation of the retentate the reaction mixture was cooled down to 5 °C, a fact which leads to a more complicated work-up procedure. The products obtained with 10 and 45 wt.% of ethanol possess similar characteristics based on GPC and elemental analysis.

**Table 3.** Overview of experiments performed with variation of alcohol amount and nature. Lignin depolymerization performed with Kraft lignin (10 wt.%), of Ru/C (0.01 wt.% metal based), alcohol (0–45 wt.%), 1 M NaOH (90–45 wt.%), 30 bar (120 barg) H<sub>2</sub> at 300 °C for 6 h.

Entry	Alcohol	NaOH (aq) Content	Soluble Retentate	Char Formation
1	-	90 wt.%	no	yes
2	10 wt.% EtOH	80 wt.%	yes (49 ± 09 wt.%)	no
3	45 wt.% EtOH	45 wt.%	yes	no
5	10 wt.% MeOH	80 wt.%	yes (18 wt.%)	no
6	10 wt.% 2-Propanol	80 wt.%	no	no
7	10 wt.% t-BuOH	80 wt.%	no	no
8	10 wt.% n-Hexanol	80 wt.%	no *	no

\* formation of two phases. The hexanol rich phase contains lignin oligomers.

Additionally, the retentate formation was significantly influenced by the nature of applied alcohol. The substitution of ethanol with methanol lead to almost triple the decrease in retentate yield (Table 3, entries 2 and 5). Obtained retentate also demonstrates slightly higher content of oxygen, suggesting incomplete hydroxy-de-oxygenation. No retentate formation was noticed by running reaction in secondary and tertiary alcohols. In case of hexanol, the formation of biphasic system after the reaction was observed. Lignin oligomers in this case are dissolved in hexanol phase (Table 3, entries 6–8).

#### 2.4. Effect of Gas Nature and Pressure

As ethanol can be considered as a donor of hydrogen, it was interesting to see the outcome of lignin depolymerization under nitrogen atmosphere. Interestingly, the yield of retentate was significantly increased by substitution of hydrogen by nitrogen. Depolymerization under nitrogen atmosphere also resulted in higher molar masses and polydispersity index of obtained lignin oligomers (Table 4, entries 1–3). Partial substitution of H<sub>2</sub> with N<sub>2</sub> also leads to a slight increase in molar mass and polydispersity index (Table 3, entries 1,2,4). Elemental analysis confirms similar composition of the obtained retentate. In addition, no nitrogen incorporation into oligomer structure took place for experiments performed under N<sub>2</sub>.

**Table 4.** Characteristics of retentates obtained by lignin depolymerization under different gas atmosphere. Lignin depolymerization performed with Kraft lignin (10 wt.%) at 300 °C for 6 h in the presence of Ru/C catalyst (0.01 wt.%, metal based), ethanol (10 wt.%), 1–30 bar (90–120 barg) of H<sub>2</sub>/N<sub>2</sub> and 1 M NaOH (80 wt.%). DMSO + LiBr was used as an eluent for GPC.

Entry	Gas	Pressure	M <sub>n,r</sub> g mol <sup>-1</sup>	M <sub>w,r</sub> g mol <sup>-1</sup>	PDI	Yield of Retentate, %
1	H <sub>2</sub>	30 bar (120 barg)	539 ± 31	1247 ± 116	2.1 ± 0.1	49 ± 09
2	N <sub>2</sub>	30 bar (120 barg)	550	1290	2.3	70
3	N <sub>2</sub>	1 bar (90 barg)	678	1680	2.5	70
4	H <sub>2</sub> + N <sub>2</sub> (1:1)	30 bar (120 barg)	542	1270	2.4	41

The obtained results suggest that lignin depolymerization precedes presumably by base-catalyzed depolymerization mechanism rather than by reductive depolymerization. On the contrary to base catalyzed mechanism, where the depolymerization proceeds through the formation of epoxide and episulfide-intermediates, in the reductive mechanism the cleavage of β-O-4 moieties happens through the direct hydrogen transfer from the catalyst. From this point of view the presence of hydrogen in the system would be beneficial in case of reductive depolymerization and should lead to a higher amount of product, which was not observed in our experiment. Furthermore, the higher amount of product was obtained in the absence of H<sub>2</sub>, suggesting that H<sub>2</sub> limits the process of retentate formation.

#### 2.5. Effect of Base Concentration

The effect of base concentration was studied by performing reaction with more diluted 0.3 M NaOH concentration in contrary to standard reaction conditions were 1.0 M NaOH was applied. In this case 6.0 g of precipitated product (60% yield) was obtained, which was slightly higher than in reaction with 1.0 M NaOH (51% yield). The obtained product also showed slightly lower molar mass and PDI (Table 5, entry 1 and 2).

**Table 5.** Characteristics of retentates obtained by lignin depolymerization with different base concentrations. Lignin depolymerization performed with Kraft lignin (10 wt.%) at 300 °C for 6 h in the presence of Ru/C catalyst (0.01 wt.%, metal based), ethanol (10 wt.%), 30 bar (120 barg) of H<sub>2</sub>, and 0.3–1 M NaOH (80 wt.%). DMSO + LiBr was used as an eluent for GPC.

Entry	Base	Lignin Content	M <sub>n,r</sub> g mol <sup>-1</sup>	M <sub>w,r</sub> g mol <sup>-1</sup>	PDI	O/C	Yield of Retentate, %
1	1.0 M NaOH	10 wt.%	527	1170	2.2	0.17	59
2	0.3 M NaOH	10 wt.%	480	956	2.0	0.17	60

#### 2.6. Effect of Reaction Time

To study the kinetics of lignin depolymerization, the monitoring of lignin oligomer precipitate formation over reaction time was performed at 300 °C using Ru/C catalyst under 30 bar (120 barg) of H<sub>2</sub>. The oligomers obtained at different reaction time were analyzed by GPC and elemental analysis. Interestingly, no product oligomer precipitation

was found after 0.5 h of depolymerization and only 14 wt.% lignin oligomer precipitate was formed within 3 h. Performing the reaction for 6 h resulted in significant yield of oligomer precipitate (51 wt.%). However, the next increase of depolymerization time led only to slight increase in product yield from 51 wt.% for 6 h to 55 wt.% for 12 h (Figure 6A). In conclusion, 6 h of reaction time was found to be optimal. On the contrary, monitoring the molar mass distribution of the lignin solution and the precipitated oligomers over the reaction time (Figure 6B) shows that significant depolymerization of the starting Kraft lignin happens already within the first 0.5 h, when no precipitation of lignin oligomers could be observed. This suggests that oligomer formation proceeds through a two-step process, in which the first step is related to lignin depolymerization and the second to the formation of a precipitating product.

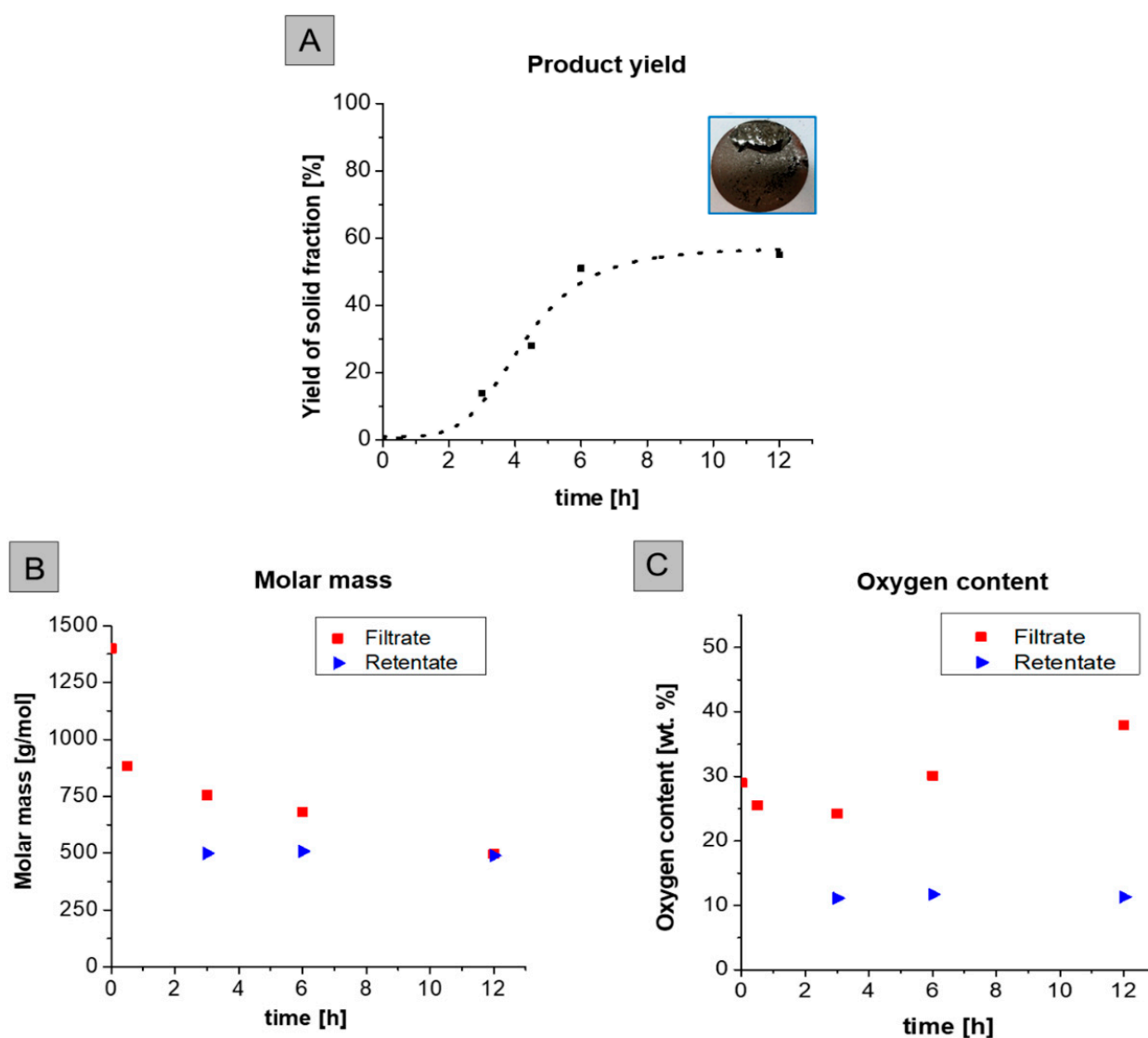


**Figure 6.** Insights into Kraft lignin depolymerization kinetics represented by the dependency of retentate yield within reaction time (A), molar mass (B), and oxygen content (C) of retentate and filtrate (NaOH phase) evolution within the reaction time.

It was also noticed that molar mass and oxygen content of precipitate (Figure 6C) remains constant during reaction time. This suggests that lignin oligomers start to precipitate out from the reaction solution, given that specific characteristics like molar mass and O-content are reached. Based on the FTIR and NMR characterization of obtained lignin

oligomers, the decrease of O content could be a result of deoxygenation by cleavage of methoxy groups.

The fact that the molar mass of the organic depolymerization products in solution changes drastically from 1400 g/mol to 870 g/mol within the first 0.5 h of reaction suggests that cleavage of ether linkages happens somewhere in the middle of the polymer chains ('reverse polycondensation' mechanism) rather than at the end of the chains, as would be expected in case of 'reverse chain-growth polymerization'.

The effect of reaction temperature and lignin concentration on yield, characteristics of the retentate as well as char formation was also investigated (Tables S1 and S2; Figure S1).

### 2.7. Elucidation of Reaction Mechanism

The significant increase of aliphatic peaks in NMR spectra of 'lignin oligomer', in comparison with the starting Kraft lignin, suggests that ethanol could react with the products obtained from lignin depolymerization. Indeed, under alkaline conditions Ru/C is a catalyst of ethanol dehydrogenation that leads to formation of highly reactive acetaldehyde [57]. To investigate the possibility of condensation of in situ formed acetaldehyde with lignin depolymerization product, the reaction with labelled  $^{13}\text{C}$ -ethanol was performed and precipitated lignin oligomers were analyzed by  $^1\text{H}$ - $^{13}\text{C}$  NMR. The obtained HSQC NMR (Figure 7) reveals the presence of new peaks in the region  $\delta_{\text{C}}/\delta_{\text{H}}$  38–42/3.5–4.2 ppm. Those peaks are expected to be related to the formation of  $-\text{CH}(\text{CH}_3)-$  bridges resulting from condensation of acetaldehyde with phenolic units. This is also confirmed by dept NMR that proves the newly formed peak to be  $\text{CH}/\text{CH}_3$  groups. It is assumed that peaks in this region are related to different o-o, o-m, m-m', or even o-p and p-p' isomers. In confirmation of the proposed mechanism, 1-butanol as condensation product of acetaldehyde was detected in the reaction media by GC-MS. Besides the fact that Ru/C is a well-known catalyst for alcohol dehydrogenation, its activity in the presence of 30 bar (120 barg) of  $\text{H}_2$  was not expected. Panchenko et al. have reported that in alkaline conditions at 180 °C and under 10 bars of  $\text{H}_2$  Ru/C is capable of dehydrogenating n-pentanol; however, the conversion was low (up to 5 mol %) [58]. It was also shown that substituting  $\text{H}_2$  with  $\text{N}_2$  resulted in 10-fold increase in reaction rate, as the presence of  $\text{H}_2$  shifts equilibrium towards alcohol formation. This agrees with our experimental results of lignin depolymerization under different gas atmosphere. (Section 2.3 effect of gas nature and pressure). Taking into consideration that acetaldehyde reacts with lignin derivatives with formation of lignin oligomers, the addition of  $\text{H}_2$  to the system based on Le Chatelier's principles would slow down the alcohol dehydrogenation reaction that would lead to decreased product yields. This can explain significantly higher yields of oligomer products in cases when lignin depolymerization is performed under nitrogen atmosphere (Table 4). Additionally, the rate of dehydrogenation increases significantly in the presence of a strong base like NaOH, due to shift of equilibria by consumption of formed aldehyde in aldol condensation with formation of Guerbet alcohol [58]. This agrees with the observation of higher molar mass of lignin oligomers obtained by using higher concentrated solutions of NaOH.

The experiment with  $^{13}\text{C}$ -labelled ethanol together with detailed parameter studies permit us to make a first assumption of the reaction pathway and the role of each component in precipitated lignin oligomers (retentate) formation (Figure 8). The first step of the process is based on catalyzed lignin depolymerization (NaOH plays a role of the catalyst for depolymerization) that proceeds through breaking ether linkages by an 'inverse polycondensation' mechanism (presumably through the formation epoxide or episulfide-intermediates [23]), and this in turn leads to the formation of lignin monomers and lignin fragments. Under alkaline condition lignin monomers existing in the form of quinone methide intermediate that are highly reactive can undergo condensation with each other, a reaction that leads to char formation [23]. This explains the char formation in reactions performed without addition of EtOH. In case of addition of an alcohol to the NaOH solution, the obtained lignin monomers/fragments can participate in condensation reactions with acetaldehyde formed in situ by ethanol dehydrogenation on Ru/C catalyst. In such a way

the main role of the metal-based catalyst in this process is dehydrogenation of alcohol with acetaldehyde formation, quenching active quinone methide intermediates by formation of lignin oligomer product. Thus, precipitated lignin oligomers have a structure similar to phenol-formaldehyde resins. The fact that molecular size of retentate is not exceeding 600 g/mol is probably related to the low solubility of formed phenol-acetaldehyde resin in alkaline water solutions that results in precipitation of lignin oligomers.

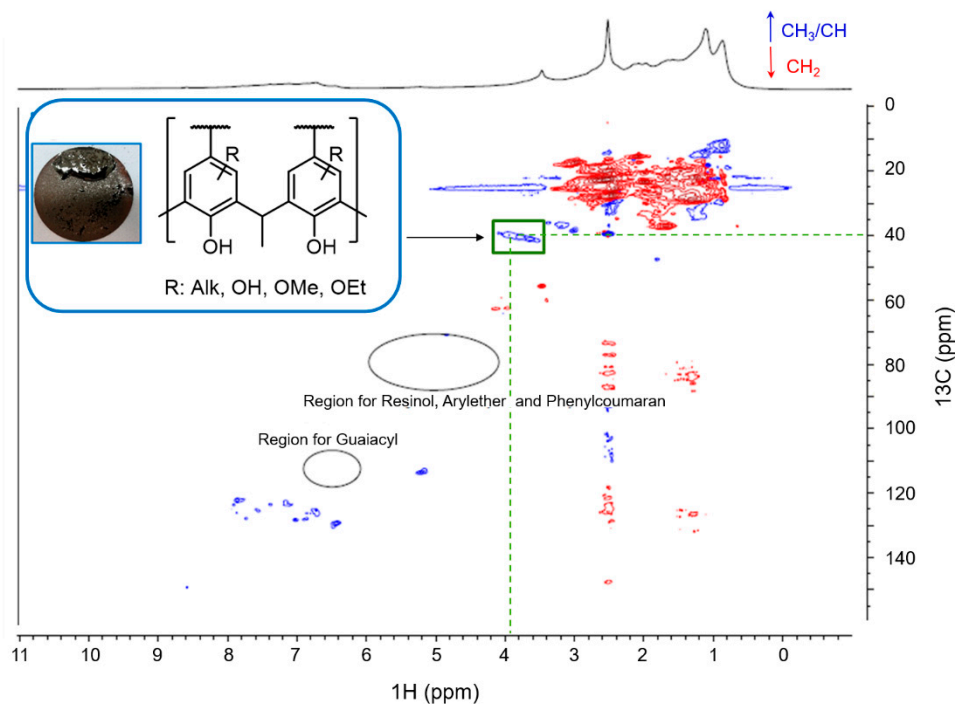


**Figure 7.**  $^1\text{H}$ - $^{13}\text{C}$  HSQC NMR spectrum precipitated lignin oligomers (retentate) obtained by performing lignin depolymerization with addition of  $^{13}\text{C}$ -labelled ethanol.

In addition, Ru/C could also participate in hydrogenation of double bonds of p-coumaryl, coniferyl, and synapyl alcohols that are known to be formed during lignin depolymerization.

### 2.8. Recycling and Characterization of Spent Catalyst

For a later industrial application, it is highly desirable to carry out reactions under low pressure and without potentially explosive gases. The use of low pressure not only prolongates the cost of equipment but also decreases the potential hazards. Recycling tests were performed in a regime relevant for industrial realization by applying 1 bar of  $\text{N}_2$  pressure (90 barg) at 300 °C for 6 h. The recycling of catalyst and NaOH solution was performed as for any industrial application, and the formation of large amounts of NaOH waste should be avoided. Thus, the recycling of NaOH solution can be regarded as beneficial for process cost reduction.

In a typical experiment the reaction solution (filtrate) obtained after the first cycle, recovered Ru/C catalyst, fresh portion of ethanol, and lignin were used for the second cycle. To keep the concentration of lignin in both cycles equal the new portion of lignin equal to the mass of recovered product in the first catalytic cycle was added to the reaction mixture. As a result, in both cycles similar amounts of oligomer products were obtained. Interestingly the products obtained in the second cycle were found to have lower molar mass, PDI, and O/C ratios (Table 6). Further recycling leads to decrease of the product yield and buildup of char, which became very pronounced already on the fourth cycle. This probably results from the accumulation of lignin fragments with high oxygen content in the filtrate fraction.

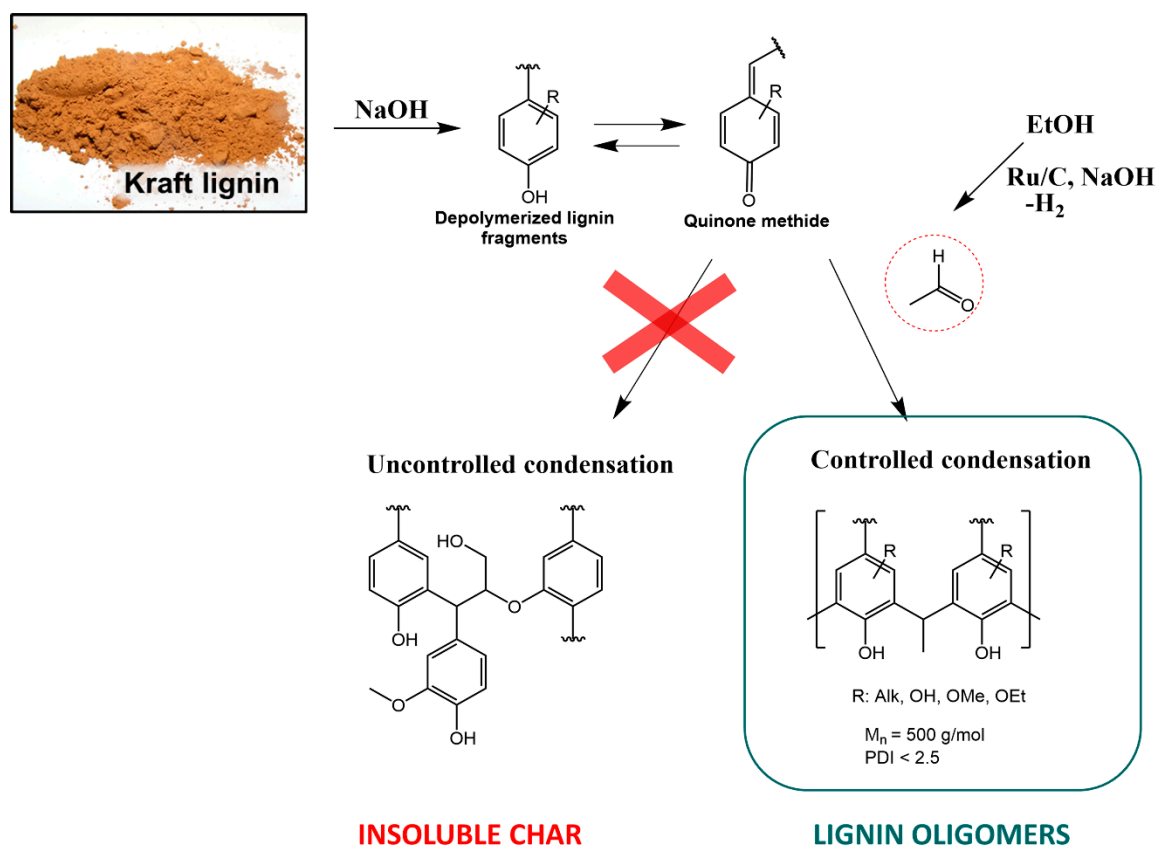


**Figure 8.** Proposed mechanism of Kraft lignin depolymerization.

**Table 6.** Characteristics of retentates obtained in recycling experiment. Lignin depolymerization performed under 1 bar (90 barg) of  $\text{N}_2$  at  $300^\circ\text{C}$  for 6 h.

Entry	Cycle	$M_{nr}$ $\text{g mol}^{-1}$	$M_{wr}$ $\text{g mol}^{-1}$	PDI	O/C	Yield of Retentate, %
1	I	678	1680	2.5	0.18	70
2	II	504	1060	2.1	0.14	66

In general, different recycling procedures showed that Ru/C catalyst as well as NaOH fraction can be recycled under standard experiment conditions under both  $\text{H}_2$  and  $\text{N}_2$  atmosphere; however, the higher product yield could be found in case of 1 bar of  $\text{N}_2$ . The EtOH used for product dissolution for catalyst recovery could be easily recovered by thermal separation.

The spent catalysts which recovered from the separate reactions of lignin depolymerization under nitrogen or hydrogen atmosphere (30 bar, 120 barg) were analyzed by elemental analysis. In both cases the final content of Ru was decreased twice (2.4 wt.% and 2.6 wt.% for reaction performed under nitrogen and hydrogen atmosphere correspondingly) in comparison with fresh catalyst that contains 5 wt.% of Ru. Meanwhile, the Ru content of filtrate fraction was lower than 1 ppm, suggesting that no leaching of Ru NPs into reaction solution take place. The elemental analysis also reveals an increase of oxygen content in the catalyst that suggests that the decrease of Ru amount is rather associated with the buildup of char on the surface of the catalyst. To clarify this point, the XPS characterization of spent catalyst was performed (Figure 9). The penetration depth of X-Rays in XPS analysis is in the range of 10 nm; thus, this technique is ideal for surface analysis. Indeed, significant difference could be found between fresh and used catalysts. The signal attributed to  $\text{RuO}_2$  species at 281.2 eV previously visible in the XPS spectrum of fresh catalyst is completely

absent in the case of the used catalyst. Under the applied reaction conditions, it is concluded that  $\text{RuO}_2$  can easily be reduced to the metallic state. However, only weak signals that could be attributed to Ru (0) at 280.2 eV can be observed in the spectrum of used catalyst. Taking into consideration that no leaching of Ru was detected, the decrease of Ru signal in the used catalyst can be only easily explained by the buildup of char on the surface of the catalyst. The presence of char precludes correct analysis of Ru species due to the limits of penetration depth of XPS method. As a confirmation of this theory the increase of C-O signal at 286.4 eV that could be attributed to ether linkages of lignin is observed in the spectrum of the spent catalyst.

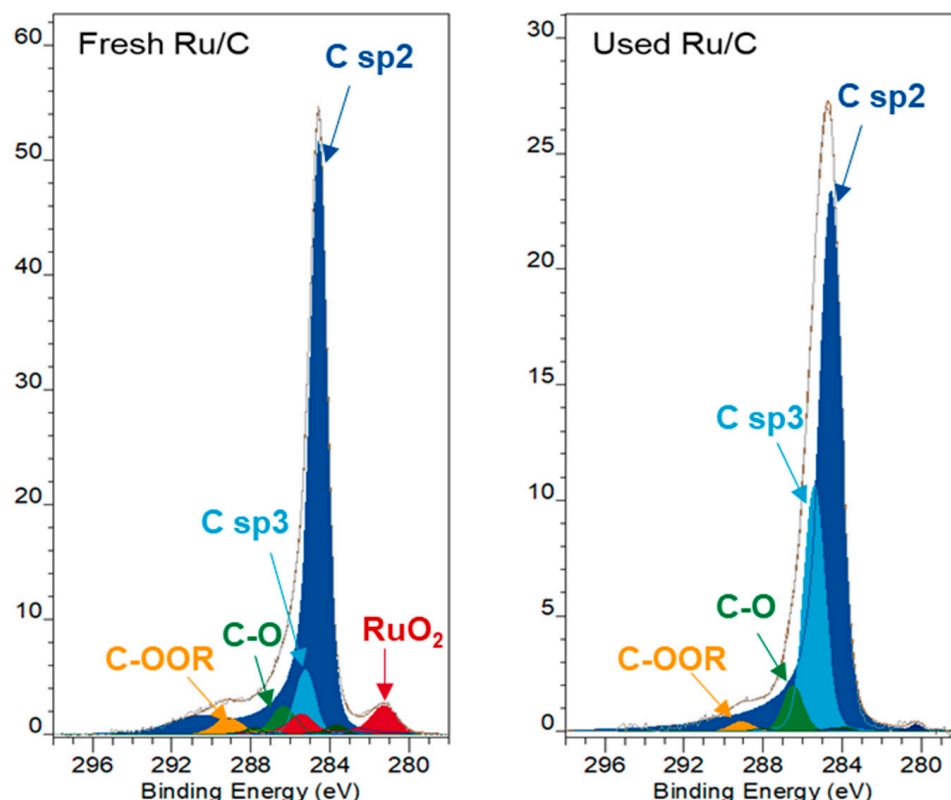


**Figure 9.** XPS spectrum of fresh and used Ru/C catalyst.

In addition to Ru, C, and O, the weak signal of sulphur could be determined in XPS spectrum. The quantification of sulphur on the surface of the used catalyst was determined to be 1.1 wt.%, which is twice as high as in the fresh catalyst. The sulfur content of starting lignin is in the range of 2–3 wt.%. Taking into consideration that 10 g of lignin and 260 mg of Ru/C catalyst were used for depolymerization, the sulfur content on the catalyst is very low. In addition, GC-MS analysis of the gas phase reveals the intensive peak of  $\text{H}_2\text{S}$ . This suggests that main mechanism of catalyst deactivation is rather related to buildup of coke on the catalyst surface, not the sulfur poisoning of the catalyst. It is also in agreement with the fact that more coking was observed while using Ru/C for more than two cycles.

### 3. Materials and Methods

#### 3.1. General

The softwood Kraft lignin used in this study was provided by the Research Institutes of Sweden and was obtained from the black liquor by Lignoboost process. Sample contained 0.76 wt.% of ash and 2.7 wt.% of sulphur.

All reagents and solvents were used without further purification. NaOH ( $\geq 99.0\%$  purity) and 2-Propanol ( $\geq 99.8\%$  pure for analysis) were purchased from Merck. Ethanol ( $\geq 99.8\%$ , absolute) was received from VWR chemicals. Dichloromethane (HPLC grade), 2,3-

Dihydrobenzofuran ( $\geq 99\%$  pure for analysis), Toluene ( $\geq 99.8\%$ , anhydrous), Ru/C catalyst (5 wt.% of Ru metal), and Nickel Nanoparticles ( $\geq 99\%$  Ni, average particle size  $< 100$  nm) were purchased from Sigma-Aldrich. Furthermore, 1 M solution of NaOH was prepared by dissolution of 40 g of NaOH pellets in 1 L of distilled water (pH = 14).

### 3.2. Catalytic Depolymerization Process

The experiments for lignin depolymerization were carried out at a temperature range of 250–350 °C in a 300 mL stainless-steel autoclave (Parr Instrument) equipped with mechanical stirrer and external heating unit. The autoclave is connected to the house hydrogen and nitrogen supply and is secured with pressure relief valve (relief pressure: 200 bar). Temperature and pressure inside the autoclave-body are detected by sensors and graphically displayed. Detailed description of the setup could be found in the Figure A4.

In a typical experiment the autoclave is filled with 10–30 wt.% of Kraft lignin, heterogeneous catalyst (1–5 wt.% in regard to lignin weight), 0–20 wt.% of alcohol, and 70–90% of 1 M NaOH solution. Afterwards, the autoclave is surely sealed and stirring speed is adjusted to 100 rpm. In order to remove air, the autoclave was subjected to three consecutive pressurization-relief cycles with 30 bars of nitrogen. Then the autoclave was filled with 30 bars of H<sub>2</sub> and heating was switched on. When the desired temperature was reached, the stirrer was slowly set to 2000 rpm. From this point, the reaction time was counted. After performing reaction for 0.5–12 h the autoclave was cooled down to room temperature and depressurized.

### 3.3. Product Work-Up

The developed work-up procedure for separation of obtained lignin oligomers is presented in Scheme 1. After lignin depolymerization the autoclave contained solid (retentate) and liquid products (NaOH fraction). In order to separate the liquid phase, the mixture was filtrated through paper filter using Buchner apparatus. The isolated liquid NaOH Fraction was divided into two parts, one of which was further used for the GPC and elemental analysis. The other part of NaOH fraction (40 mL) was further neutralized by HCl till pH = 2 followed by extraction with chloroform (5 mL). The extracted phase was further analyzed by GC-MS for the monoaromatic content. The recovery of lignin phase dissolved in NaOH was not successful.

The retentate isolated on the paper filter after first filtration step consisted of catalyst, char, and lignin oligomers product. To separate lignin oligomers from char and catalyst the mixture was washed on filter with 100 mL of ethanol. In order to isolate maximum amount of lignin oligomers products that tend to stick to the internal parts of the autoclave, the autoclave and stirrer were also washed with ethanol and this solution was further used for washing of retentate collected on the filter. Lignin oligomers are soluble in ethanol and were isolated as a liquid phase while catalyst and char stayed on the filter. The recovered catalyst and char were left to dry on paper filter overnight. The amount of char was determined as a weight difference between recovered solid and amount of catalyst used in the reaction. Lignin oligomers were isolated as solid material after evaporation of ethanol in rotary evaporator. The yield of lignin oligomers was determined as a mass of obtained dried lignin oligomers to the mass of starting Kraft lignin in percentages.

#### 3.3.1. Recycling

In the recycling experiments the recycling of both NaOH solution and Ru/C catalyst was performed simultaneously. For this, liquid NaOH fraction collected in the first cycle (86 g) was mixed with dried, washed Ru/C collected after the first reaction cycle (240 mg), fresh portion of EtOH (10 mL), and fresh portion of Kraft lignin. To keep the lignin concentration in NaOH solution similar as in the first cycle, the amount of fresh lignin added to the solution was equal by mass of retentate obtained in the first cycle (5 g). The mixture was transferred to the autoclave and the reaction proceeded under 30 bar of N<sub>2</sub> (initial pressure) at 300 °C for 6 h. After the work-up and isolation of NaOH fraction, an

aliquot (0.5 mL) of NaOH liquid fraction was withdrawn from the solution and sent to the GPC analysis and the liquid was used for the next cycle. Obtained retentate was analyzed by GPC and elemental analysis as previously described. The attempts to perform recycling experiments with Ni based catalyst resulted in a huge amount of char.

### 3.3.2. GPC Analysis

GPC analysis is performed using Agilent PolarGel M columns in DMSO/LiBr as solvent. Intensities are recorded by a UV-Vis detector (Agilent 1200 VWD 232 nm) and refractive index detector (DRI Agilent 1200 UV). Elution temperature is 35 °C, flow rate is 0.5 mL/min. For DMSO + 0.5%LiBr SEC calibration is carried out with narrowly distributed polystyrene sulfonate standards from the company PSS with molecular weights of  $M = 208$  to  $M = 152,000$ .

GPC analysis of the residues (the lignin oligomers) which usually are dissolved in EtOH is performed using Agilent PolarGelM columns in DMSO/LiBr as solvent. Intensities are recorded by a UV-Vis detector (Agilent 1200 VWD 232 nm) and refractive index detector (DRI Agilent 1200 UV). Elution temperature is 35 °C, flow rate is 0.5 mL/min. For DMSO + 0.5%LiBr SEC calibration was carried out with narrowly distributed polystyrene sulfonate standards from the company PSS with molecular weights of  $M = 208$  to  $M = 152,000$ . Samples were dissolved in eluent and filtered using a 0.2 µm membrane (Sartorius RC 25) before analysis.

### 3.3.3. Elemental Analysis

Elemental analysis was performed from freeze-dried samples to remove residual water and solvent. Carbon, hydrogen, nitrogen, and sulfur analysis is conducted by combustion followed by thermal conductivity and infrared detection of effluent gases. Sulfur effluent gases are adsorbed in hydrogen peroxide solution and the resulting sulfuric acid is titrated with alkali base. The oxygen content is determined by considering proportional formula for organic compounds containing C, H, and O. Ru amount was determined by ICP analysis.

### 3.3.4. GC-MS

GC-MS analyses were executed on an Agilent 6890 A GC-chromatograph with connected mass spectrometer (Agilent 5973). A VF-5 ht column with 30 m of length, 0.25 mm inner diameter, and 0.1 µm film thickness was used as stationary phase. Before analysis the filtrate containing NaOH and fragments of lignin was neutralized with HCl to pH = 2 and further extracted with chloroform. Obtained organic phase was filtered over PTFE syringe filter (0.1 µm). Then, 0.9 mL of the resulting filtrate was mixed with 0.1 mL ethanol containing toluene and 2,3-dihydrobenzofuran as internal standards (10 g/L).

### 3.3.5. FTIR Analysis

FT-IR spectra of Kraft lignin (starting material) and lignin oligomer were reordered with Alpha-T Transmission FT-IR (MIR) Spectrometer equipped with universal sample module. Solid samples were deposited on a single ZnSe optical window and measured in spectral range of 600–4000  $\text{cm}^{-1}$  in a transition mod.

### 3.3.6. NMR

All NMR spectra were recorded using a 700 MHz Bruker AV700 spectrometer. For  $^1\text{H}$ -NMR, approximately 100 µL of samples in NaOH (1M) were mixed with 400 µL  $\text{D}_2\text{O}$  and measured under water signal-suppression. For  $^1\text{H}$ - $^{13}\text{C}$  HSQC and HMBC NMR spectra, samples were freeze-dried and dissolved in deuterated DMSO with 200 mg/mL. TMS was used as internal standard.

### 3.3.7. XPS

The XPS analyses were carried out with a PHI Quantum 2000 XPS-Spectrometer (Physical Electronics, Chanhassen USA) using monochromatic Al K $\alpha$  radiation (50 W) with a spot size of 200  $\mu$ m diameter in standard configuration. The XPS system was calibrated according to ISO 15472:2001. The BE (Binding Energy) of Au 4f $_{7/2}$  was 84.00 eV and that of Cu 2p $_{3/2}$  was 932.62 eV. All samples were mounted insulated against ground and neutralized during the measurements with the built-in charge neutralizer. Survey scan analyses were carried out with a pass energy of 117.4 eV and an energy step size of 0.5 eV. High resolution analyses were carried out on the same analysis area with a pass energy of 23.5 eV and an energy step size of 0.1 eV. Spectra have been charge corrected to the main line of the carbon 1s spectrum set to 284.5 eV as a typical value quoted for aromatic carbon. All spectra were analyzed using the XPS-analysis software CasaXPS using Shirley background subtraction of the main peaks for the elements of interest (C 1s, Cr 2p, Fe 2p, In 3d $_{5/2}$ , Na 1s, O 1s, Ru 3p $_{3/2}$ , S 2p, Si 2p). Relative sensitivity factors and transmission function as provided by the instrument manufacturer were used for quantification.

## 4. Conclusions

In summary, we have demonstrated a simple method to obtain lignin oligomers with low molar mass of 600 g/mol and moderate polydispersity  $2.1 \pm 0.1$  from Kraft lignin by combination of base-catalyzed and reductive depolymerization strategy under non-oxidative atmosphere at 300 °C. At present the high temperatures coupled with the high base concentrations pose some challenges regarding corrosion for the realization on the industrial scale, but the process benefits from high yield (of up to 70 wt.%) and easy recovery of product, as well as absence of char formation. It was found that presence of catalyst, alcohol, base, and non-oxidative gas are all required for precipitation of lignin oligomers out of solution. The influence of catalyst, alcohol, reaction atmosphere, reagents concentration reaction temperature, and reaction time on the yield and composition of lignin oligomers was studied in detail. The most pronounced effects were found in case of the reaction temperature, reaction time, and applied atmosphere. In such a way the temperatures <250 °C do not lead to formation of product, while too high temperatures >330 °C lead to extended char formation. Kinetic measurements show that reaction time of 6 h is the optimum; performing the reaction for less time results in a significant decrease of product yield. It was also found that yield of lignin oligomers significantly increased when N $_2$  was used instead of H $_2$ ; however, all lignin oligomers obtained by applying different reaction conditions show similar elemental composition. The detailed characterization of obtained oligomers confirms significant depolymerization and hydrodeoxygenation of initial Kraft lignin. Obtained lignin oligomers show more homogeneous structure in terms of chemical composition in comparison with starting Kraft lignin. It was also found that ethanol in combination with a hydrogenation/dehydrogenation catalyst like Ru/C is responsible for char suppression. In particular, the experiment with  $^{13}$ C-labelled ethanol proves that alcohol reacts with depolymerized lignin fragments with the formation of phenol-formaldehyde resin like product. We hypothesize that the main role of the catalyst in this process is to convert ethanol into highly reactive acetaldehyde that can further quench active quinone methide intermediates that tend to repolymerize. The detection of Guerbet products by GC-MS also supports the proposed theory. Finally, the catalyst, NaOH in the form of the filtered solution and ethanol used for product dissolution can be recycled. It should be mentioned that recycling of the Ru/C catalyst more than two times leads to partial loss of catalytic activity due to the buildup of a char on the catalyst surface as it was shown by XPS. Meanwhile, the results of gas phase analysis suggest that poisoning of active sites by sulfur is rather unlikely as the biggest part of it is transferred into gas phase in the form of H $_2$ S.

## 5. Patents

The work is summarized in the patent application 191530EP: Method for preparation of Lignin Oligomers.

**Supplementary Materials:** The following supporting information can be downloaded at: <https://www.mdpi.com/article/10.3390/catal12020158/s1>, Figure S1: Effect of lignin concentration on yield of lignin oligomers product normalized by dissolved amount of lignin, Figure S2:  $^{31}\text{P}$  NMR spectrum of Lignin oligomers and starting Kraft lignin, Reference [59] are cited in the supplementary materials. Table S1: Effect of temperature on formation lignin oligomers and char, Table S2: Characteristics of retentates obtained by lignin depolymerization with lignin concentrations, Table S3: Distribution of aromatic and aliphatic OH in the starting Kraft lignin and lignin oligomers obtained under standard conditions.

**Author Contributions:** Conceptualization, I.R., J.-P.L. and S.A.S.; data curation, I.R. and J.-P.L.; funding acquisition, A.K. (Alois Kindler) and S.A.S.; investigation, I.R., F.K., R.B. and A.K. (Arunabha Kundu); project administration, J.-P.L. and S.A.S.; supervision, I.J., A.K. (Alois Kindler) and S.A.S.; validation, I.R., R.B. and J.-P.L.; visualization, I.R., R.B., I.J. and J.-P.L.; writing—original draft, I.R. and S.A.S.; writing—review and editing, I.R., I.J. and S.A.S. All authors have read and agreed to the published version of the manuscript.

**Funding:** Founding through BASF SE and hte GmbH is gratefully acknowledged.

**Institutional Review Board Statement:** Not applicable.

**Informed Consent Statement:** Not applicable.

**Data Availability Statement:** Not applicable.

**Conflicts of Interest:** The authors declare no conflict of interest.

## Appendix A

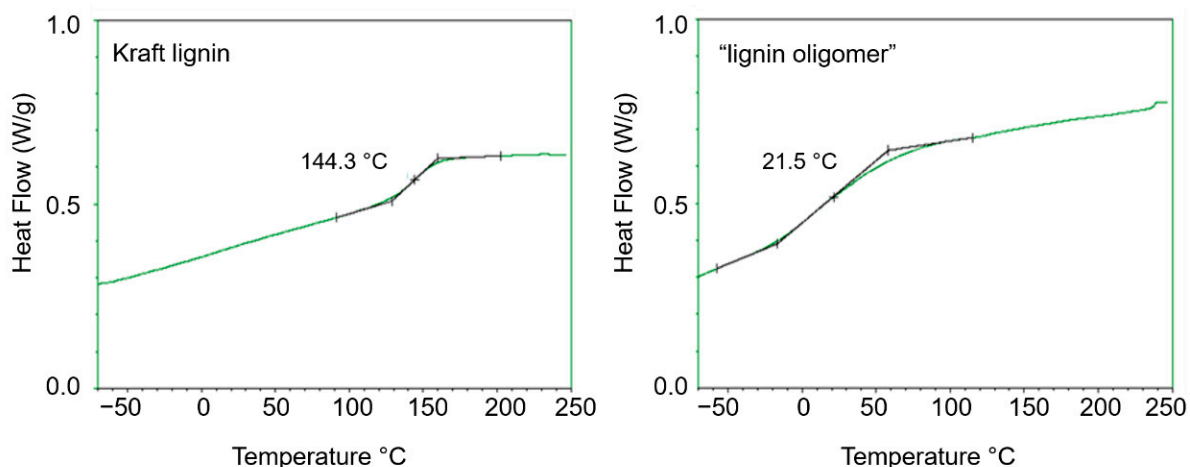


**Figure A1.** DSC thermogram of starting Kraft lignin (left) and precipitated "lignin oligomer" product (right).

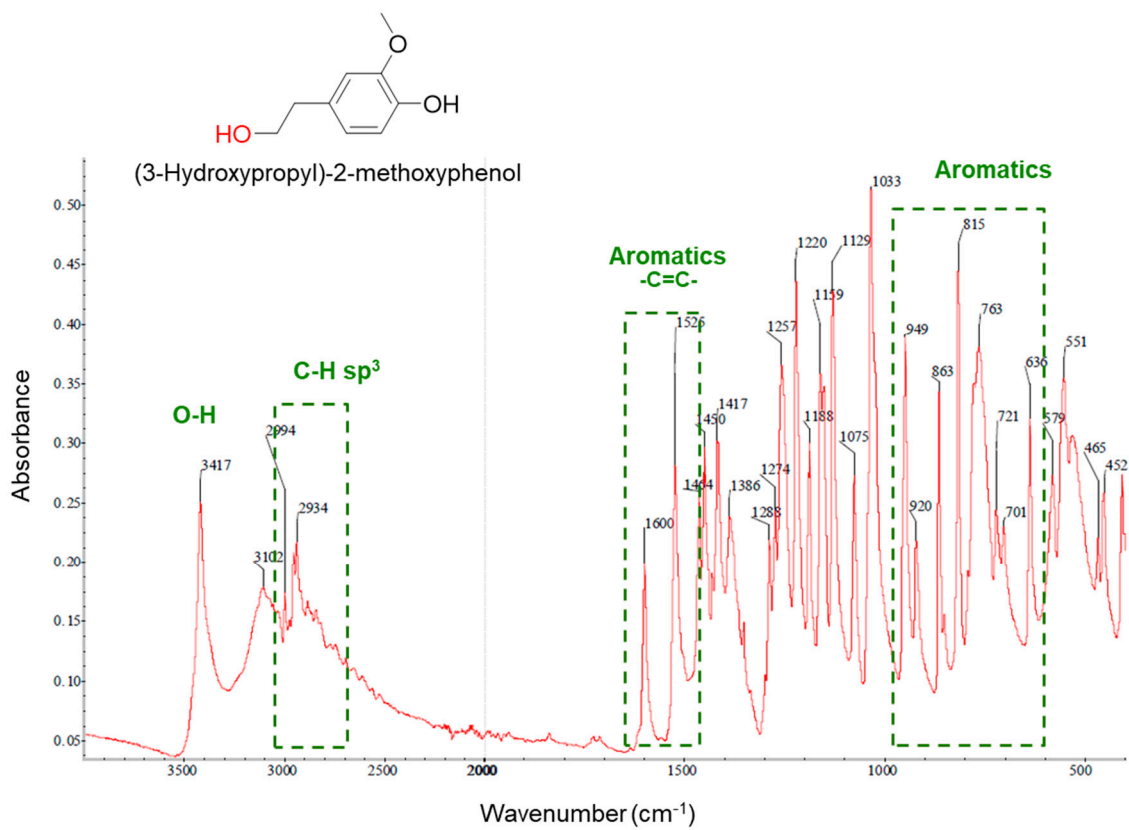


Figure A2. FTIR spectrum of (3-Hydroxypropyl)-2-methoxyphenol.

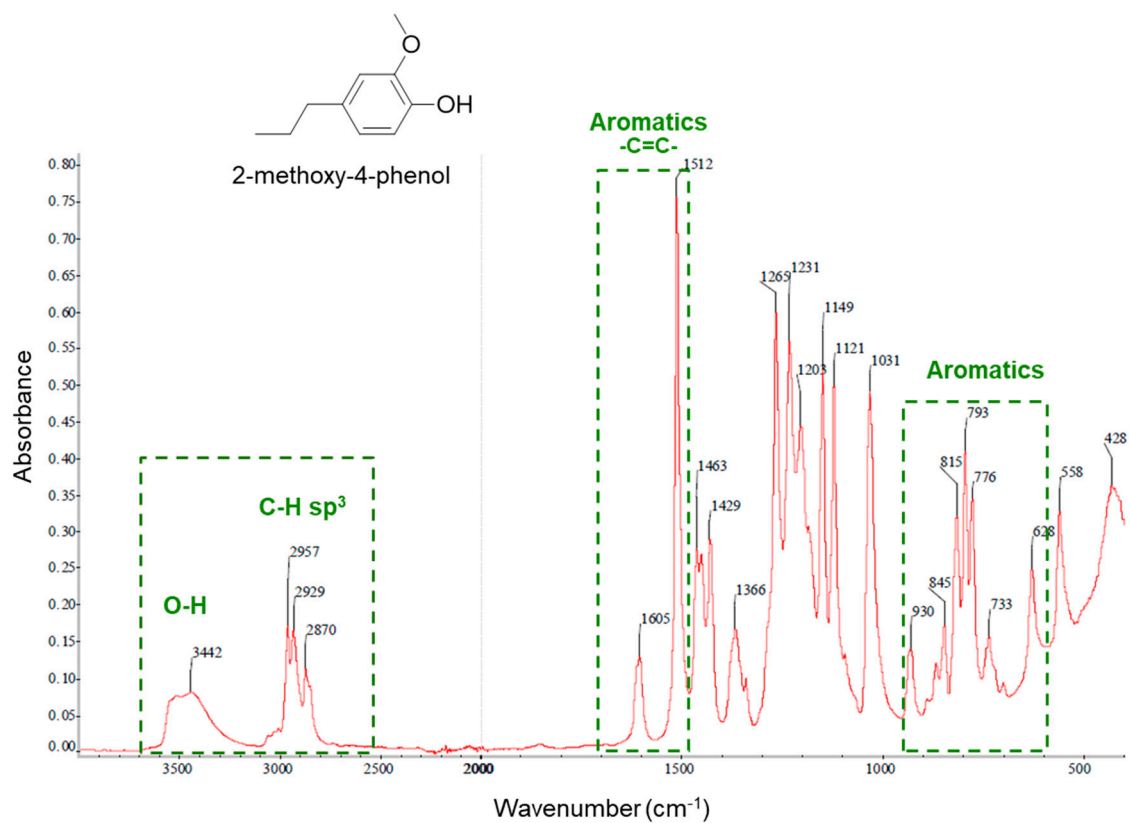


Figure A3. FTIR spectrum of 2-methoxy-4-phenol.

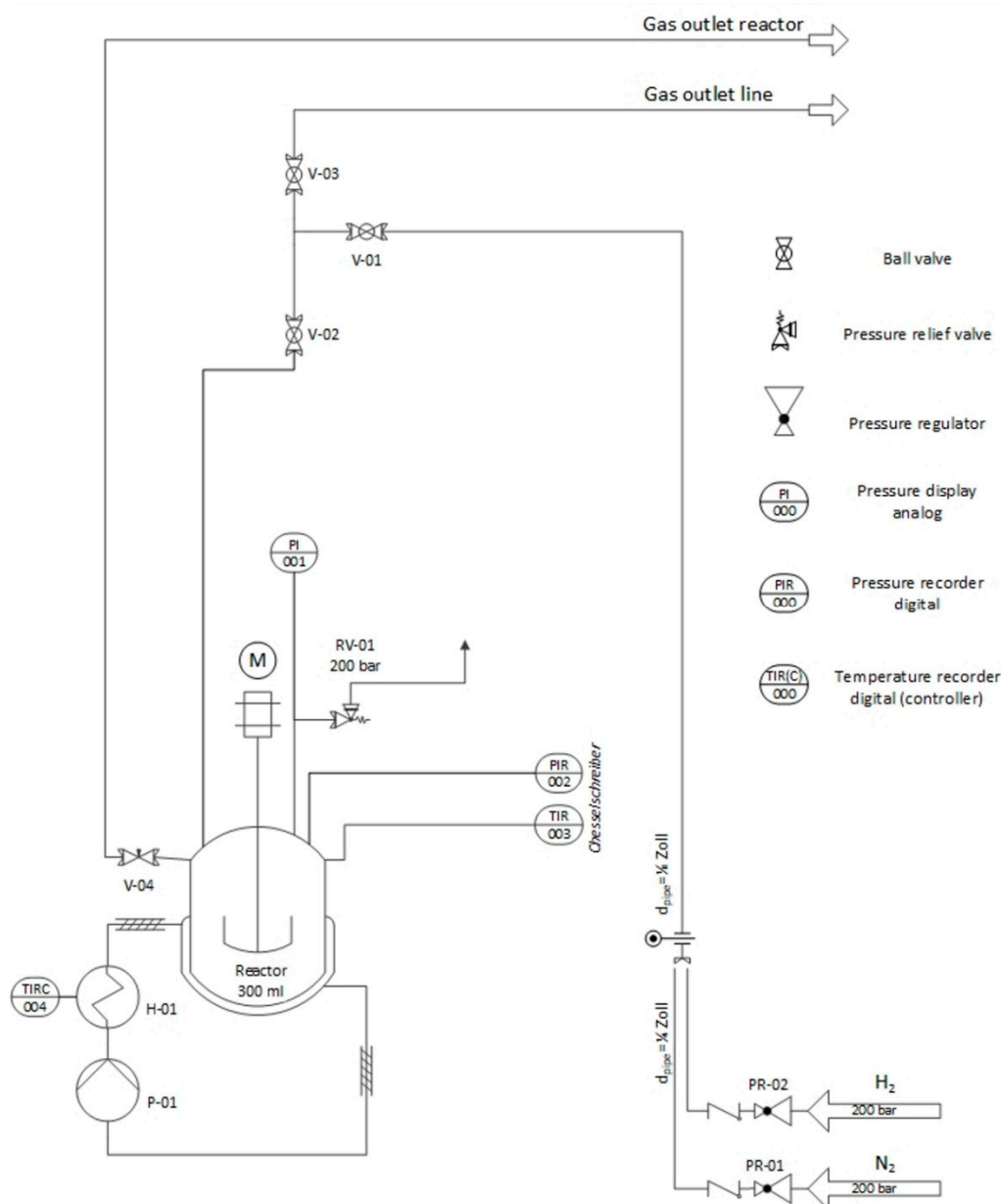


Figure A4. P&I scheme of reactor setup used for lignin depolymerization.

## References

- Huber, G.W.; Iborra, S.; Corma, A. Synthesis of Transportation Fuels from Biomass: Chemistry, Catalysts, and Engineering. *Chem. Rev.* **2006**, *106*, 4044–4098. [[CrossRef](#)] [[PubMed](#)]
- Kärkäs, M.D.; Matsuura, B.S.; Monos, T.M.; Magallanes, G.; Stephenson, C.R.J. Transition-metal catalyzed valorization of lignin: The key to a sustainable carbon-neutral future. *Org. Biomol. Chem.* **2016**, *14*, 1853–1914. [[CrossRef](#)] [[PubMed](#)]
- Pandey, M.P.; Kim, C.S. Lignin Depolymerization and Conversion: A Re-view of Thermochemical Methods. *Chem. Eng. Technol.* **2011**, *34*, 29–41. [[CrossRef](#)]
- Berlin, A.; Balakshin, M. Industrial Lignins. In *Bioenergy Research: Advances and Applications*; Elsevier: Amsterdam, The Netherlands, 2014; pp. 315–336.
- Tomani, P. The LignoBoost Process. *Cellul. Chem. Technol.* **2010**, *44*, 53–58.
- Lancefield, C.S.; Wienk, H.L.J.; Boelens, R.; Weckhuysen, B.M.; Bruijninx, P.C.A. Identification of a diagnostic structural motif reveals a new reaction intermediate and condensation pathway in kraft lignin formation. *Chem. Sci.* **2018**, *9*, 6348–6360. [[CrossRef](#)] [[PubMed](#)]
- Crestini, C.; Lange, H.; Sette, M.; Argyropoulos, D.S. On the structure of softwood kraft lignin. *Green Chem.* **2017**, *19*, 4104–4121. [[CrossRef](#)]

8. Hunter-Cevera, K.R.; Neubert, M.G.; Olson, R.J.; Solow, A.R.; Shalapyonok, A.; Sosik, H.M. Physiological and eco-logical drivers of early spring blooms of a coastal phytoplankter. *Science* **2016**, *354*, 326–329. [[CrossRef](#)]
9. Vanholme, R.; Demedts, B.; Morreel, K.; Ralph, J.; Boerjan, W. Lignin bio-synthesis and structure. *Plant Physiol.* **2010**, *153*, 895–905. [[CrossRef](#)]
10. Zhang, B.; Guo, T.; Liu, Y.; Kühn, F.E.; Wang, C.; Zhao, Z.K.; Xiao, J.; Li, C.; Zhang, T. Sustainable Production of Benzylamines from Lignin. *Angew. Chem. Int. Ed.* **2021**, *60*, 20666–20671. [[CrossRef](#)]
11. Elangovan, S.; Afanasenko, A.; Haupenthal, J.; Sun, Z.; Liu, Y.; Hirsch, A.; Barta, K. From Wood to Tetrahydro-2-benzazepines in Three Waste-Free Steps Modular Synthesis of Biologically Active Lig-nin-Derived Scaffolds Enhanced Reader. *ACS Cent. Sci.* **2019**, *5*, 1707–1716. [[CrossRef](#)]
12. Zeng, H.; Cao, D.; Qiu, Z.; Li, C.-J. Palladium-Catalyzed Formal Cross-Coupling of Diaryl Ethers with Amines: Slicing the 4-O-5 Linkage in Lignin Models. *Angew. Chem. Int. Ed.* **2018**, *57*, 3752–3757. [[CrossRef](#)] [[PubMed](#)]
13. Katahira, R.; Mittal, A.; McKinney, K.; Chen, X.; Tucker, M.P.; Johnson, D.K.; Beckham, G.T. Base-Catalyzed Depolymerization of Biorefinery Lignins. *ACS Sustain. Chem. Eng.* **2016**, *4*, 1474–1486. [[CrossRef](#)]
14. Du, X.; Li, J.; Lindström, M.E. Modification of industrial softwood kraft lignin using Mannich reaction with and without phenolation pretreatment. *Ind. Crops Prod.* **2014**, *52*, 729–735. [[CrossRef](#)]
15. Deuss, P.J.; Scott, M.; Tran, F.; Westwood, N.J.; de Vries, J.G.; Barta, K. Aromatic monomers by in situ conversion of reactive intermediates in the acid-catalyzed depolymerization of lignin. *J. Am. Chem. Soc.* **2015**, *137*, 7456–7467. [[CrossRef](#)]
16. Yuan, Z.; Tymchyshyn, M.; Xu, C. Reductive Depolymerization of Kraft and Organosolv Lignin in Supercritical Acetone for Chemicals and Materials. *ChemCatChem* **2016**, *8*, 1968–1976. [[CrossRef](#)]
17. Yu, X.; Wei, Z.; Lu, Z.; Pei, H.; Wang, H. Activation of lignin by selective oxidation: An emerging strategy for boost-ing lignin depolymerization to aromatics. *Bioresour. Technol.* **2019**, *291*, 121885. [[CrossRef](#)]
18. Hanson, S.K.; Baker, R.T. Knocking on wood: Base metal complexes as catalysts for selective oxidation of lignin models and extracts. *Acc. Chem. Res.* **2015**, *48*, 2037–2048. [[CrossRef](#)]
19. Adam, M.; Ocone, R.; Mohammad, J.; Berruti, F.; Briens, C. Kinetic Investigations of Kraft Lignin Pyrolysis. *Ind. Eng. Chem. Res.* **2013**, *52*, 8645–8654. [[CrossRef](#)]
20. Jiang, G.; Nowakowski, D.J.; Bridgwater, A.V. Effect of the Temperature on the Composition of Lignin Pyrolysis Products. *Energy Fuels* **2010**, *24*, 4470–4475. [[CrossRef](#)]
21. Kawamoto, H. Lignin pyrolysis reactions. *J. Wood Sci.* **2017**, *63*, 117–132. [[CrossRef](#)]
22. Li, C.; Zhao, X.; Wang, A.; Huber, G.; Zhang, T. Catalytic Transformation of Lignin for the Production of Chemicals and Fuels. *Chem. Rev.* **2015**, *115*, 11559–11624. [[CrossRef](#)] [[PubMed](#)]
23. Sun, Z.; Fridrich, B.; de Santi, A.; Elangovan, S.; Barta, K. Bright Side of Lignin Depolymerization: Toward New Plat-form Chemicals. *Chem. Rev.* **2018**, *118*, 614–678. [[CrossRef](#)] [[PubMed](#)]
24. Schutyser, W.; Renders, T.; Van Den Bosch, S.; Koelewijn, S.-F.; Beckham, G.T.; Sels, B.F. Chemicals from lignin: An interplay of lignocellulose fractionation, depolymerisation, and upgrading. *Chem. Soc. Rev.* **2018**, *47*, 852–908. [[CrossRef](#)] [[PubMed](#)]
25. Kim, K.H.; Dutta, T.; Walter, E.D.; Isern, N.G.; Cort, J.R.; Simmons, B.A.; Singh, S. Chemoselective Methylation of Phenolic Hydroxyl Group Prevents Quinone Methide Formation and Repolymerization During Lignin Depolymerization. *ACS Sustain. Chem. Eng.* **2017**, *5*, 3913–3919. [[CrossRef](#)]
26. Kim, K.H.; Kim, C.S. Recent Efforts to Prevent Undesirable Reactions from Fractionation to Depolymerization of Lignin: Toward Maximizing the Value from Lignin. *Front. Energy Res.* **2018**, *6*, 170. [[CrossRef](#)]
27. Klein, I.; Marcum, C.; Kenttämä, H.; Abu-Omar, M.M. Mechanistic investigation of the Zn/Pd/C catalyzed cleavage and hydrodeoxygenation of lignin. *Green Chem.* **2016**, *18*, 2399–2405. [[CrossRef](#)]
28. Zakzeski, J.; Jongorius, A.L.; Bruijninx, P.C.A.; Weckhuysen, B.M. Catalytic lignin valorization process for the pro-duction of aromatic chemicals and hydrogen. *ChemSusChem* **2012**, *5*, 1602–1609. [[CrossRef](#)]
29. Shuai, L.; Sitison, J.; Sadula, S.; Ding, J.; Thies, M.C.; Saha, B. Selective C–C Bond Cleavage of Methylene-Linked Lignin Models and Kraft Lignin. *ACS Catal.* **2018**, *8*, 6507–6512. [[CrossRef](#)]
30. Lv, W.; Si, Z.; Tian, Z.; Wang, C.; Zhang, Q.; Xu, Y.; Wang, T.; Ma, L. Synergistic Effect of EtOAc/H<sub>2</sub>O Biphasic Solvent and Ru/C Catalyst for Cornstalk Hydrol-ysis Residue Depolymerization. *ACS Sustain. Chem. Eng.* **2017**, *5*, 2981–2993. [[CrossRef](#)]
31. Shen, X.-J.; Huang, P.-L.; Wen, J.-L.; Sun, R.-C. A facile method for char elimination during base-catalyzed depolymerization and hydrogenolysis of lignin. *Fuel Process. Technol.* **2017**, *167*, 491–501. [[CrossRef](#)]
32. Long, J.; Xu, Y.; Wang, T.; Yuan, Z.; Shu, R.; Zhang, Q.; Ma, L. Efficient base-catalyzed decomposition and in situ hydrogenolysis process for lignin depolymerization and char elimination. *Appl. Energy* **2015**, *141*, 70–79. [[CrossRef](#)]
33. Hossain, A.; Phung, T.K.; Rahaman, M.S.; Tulaphol, S.; Jasinski, J.B.; Sathitsuksanoh, N. Catalytic cleavage of the B-O-4 aryl ether bonds of lignin model compounds by Ru/C catalyst. *Appl. Catal. A Gen.* **2019**, *582*, 117100. [[CrossRef](#)]
34. Wang, X.; Rinaldi, R. Solvent effects on the hydrogenolysis of diphenyl ether with Raney nickel and their implications for the conversion of lignin. *ChemSusChem* **2012**, *5*, 1455–1466. [[CrossRef](#)] [[PubMed](#)]
35. Barta, K.; Matson, T.D.; Fettig, M.L.; Scott, S.L.; Iretskii, A.V.; Ford, P.C. Catalytic disassembly of an organosolv lignin via hydrogen transfer from supercritical methanol. *Green Chem.* **2010**, *12*, 1640. [[CrossRef](#)]
36. Macala, G.S.; Matson, T.D.; Johnson, C.L.; Lewis, R.S.; Iretskii, A.V.; Ford, P.C. Hydrogen Transfer from Supercritical Methanol over a Solid Base Catalyst: A Model for Lignin Depolymerization. *ChemSusChem* **2009**, *2*, 215–217. [[CrossRef](#)]

37. Matson, T.D.; Barta, K.; Iretskii, A.V.; Ford, P.C. One-pot catalytic conversion of cellulose and of woody biomass solids to liquid fuels. *J. Am. Chem. Soc.* **2011**, *133*, 14090–14097. [[CrossRef](#)]
38. Huang, X.; Korányi, T.I.; Boot, M.D.; Hensen, E.J.M. Catalytic depolymerization of lignin in supercritical ethanol. *ChemSusChem* **2014**, *7*, 2276–2288. [[CrossRef](#)]
39. Huang, X.; Korányi, T.I.; Boot, M.D.; Hensen, E.J.M. Ethanol as capping agent and formaldehyde scavenger for efficient depolymerization of lignin to aromatics. *Green Chem.* **2015**, *17*, 4941–4950. [[CrossRef](#)]
40. Kim, J.-Y.; Park, J.; Hwang, H.; Kim, J.K.; Song, I.K.; Choi, J.W. Catalytic de-polymerization of lignin macromolecule to alkylated phenols over various metal cata-lysts in supercritical tert-butanol. *J. Anal. Appl. Pyrolysis* **2015**, *113*, 99–106. [[CrossRef](#)]
41. Kim, J.-Y.; Park, J.; Kim, U.-J.; Choi, J.W. Conversion of Lignin to Phenol-Rich Oil Fraction under Supercritical Alcohols in the Presence of Metal Catalysts. *Energy Fuels* **2015**, *29*, 5154–5163. [[CrossRef](#)]
42. Yoshikawa, T.; Yagi, T.; Shinohara, S.; Fukunaga, T.; Nakasaka, Y.; Tago, T.; Masuda, T. Production of phenols from lignin via depolymerization and catalytic cracking. *Fuel Process. Technol.* **2013**, *108*, 69–75. [[CrossRef](#)]
43. Wu, Y.; Chen, Y.; Wu, K. Role of Co-Solvents in Biomass Conversion Reactions Using Sub/Supercritical Water. In *Near-Critical and Supercritical Water and Their Applications for Biorefineries*; Fang, Z., Xu, C., Eds.; Springer: Dordrecht, The Netherlands, 2014.
44. Sebhat, W. Valorisation de la Lignine par Catalyse Hétérogène en Condition Sous-Critique en Milieux Aqueux et Eau/Alcool. PhD. Thesis, Université Claude Bernard—Lyon I, Lyon, France, 2016.
45. Saisu, M.; Sato, T.; Watanabe, M.; Adschiri, T.; Arai, K. Conversion of Lignin with Supercritical Water—Phenol Mixtures. *Energy Fuels* **2003**, *17*, 922–928. [[CrossRef](#)]
46. Roberts, V.M.; Stein, V.; Reiner, T.; Lemonidou, A.; Li, X.; Lercher, J.A. To-towards quantitative catalytic lignin depolymerization. *Chemistry* **2011**, *17*, 5939–5948. [[CrossRef](#)] [[PubMed](#)]
47. Okuda, K.; Umetsu, M.; Takami, S.; Adschiri, T. Disassembly of lignin and chemical recovery—rapid depolymerization of lignin without char formation in wa-ter–phenol mixtures. *Fuel Process. Technol.* **2004**, *85*, 803–813. [[CrossRef](#)]
48. Lee, H.; Jae, J.; Ha, J.-M.; Suh, D.J. Hydro- and solvothermolysis of kraft lignin for maximizing production of monomeric aromatic chemicals. *Bioresour. Technol.* **2016**, *203*, 142–149. [[CrossRef](#)]
49. Kang, S.; Li, X.; Fan, J.; Chang, J. Hydrothermal conversion of lignin: A review. *Renew. Sustain. Energy Rev.* **2013**, *27*, 546–558. [[CrossRef](#)]
50. Cheng, Y.; Zhou, Z.; Alma, M.H.; Sun, D.; Zhang, W.; Jiang, J. Direct Liquefaction of Alkali Lignin in Methanol and Water Mixture for the Production of Oligomeric Phenols and Aromatic Ethers. *J. Biobased Mater. Bioenergy* **2016**, *10*, 76–80. [[CrossRef](#)]
51. Cheng, S.; Wilks, C.; Yuan, Z.; Leitch, M.; Xu, C. Hydrothermal degradation of alkali lignin to bio-phenolic compounds in sub/supercritical ethanol and water–ethanol co-solvent. *Polym. Degrad. Stab.* **2012**, *97*, 839–848. [[CrossRef](#)]
52. Belkheiri, T.; Andersson, S.-I.; Mattsson, C.; Olausson, L.; Theliander, H.; Vamling, L. Hydrothermal liquefaction of kraft lignin in sub-critical water: The influence of the sodium and potassium fraction. *Biomass Convers. Biorefin.* **2018**, *8*, 585–595. [[CrossRef](#)]
53. Belkheiri, T.; Vamling, L.; Nguyen, T.; Maschietti, M.; Olausson, L.; Andersson, S.-I.; Amand, L.-E.; Theliander, H. Kraft lignin depolymerization in near-critical water: Effect of changing co-solvent. *Cellul. Chem. Technol.* **2014**, *48*, 813–818.
54. Arturi, K.R.; Strandgaard, M.; Nielsen, R.P.; Sogaard, E.G.; Maschietti, M. Hydrothermal liquefaction of lignin in near-critical water in a new batch reactor: In-fluence of phenol and temperature. *J. Supercrit. Fluids* **2017**, *123*, 28–39. [[CrossRef](#)]
55. Kaiho, A.; Kogo, M.; Sakai, R.; Saito, K.; Watanabe, T. In situ trapping of enol intermediates with alcohol during acid-catalysed de-polymerisation of lignin in a nonpolar solvent. *Green Chem.* **2015**, *17*, 2780–2783. [[CrossRef](#)]
56. Wang, X.; Wang, N.; Nguyen, T.T.; Qian, E.W. Catalytic Depolymerization of Lignin in Ionic Liquid Using a Continuous Flow Fixed-Bed Reaction System. *Ind. Eng. Chem. Res.* **2018**, *57*, 16995–17002. [[CrossRef](#)]
57. Gabriëls, D.; Hernández, W.Y.; Sels, B.; van der Voort, P.; Verberckmoes, A. Review of catalytic systems and thermodynamics for the Guerbet condensation reaction and challenges for biomass valorization. *Catal. Sci. Technol.* **2015**, *5*, 3876–3902. [[CrossRef](#)]
58. Panchenko, V.N.; Paukshtis, E.A.; Murzin, D.Y.; Simakova, I.L. Solid Base Assisted n -Pentanol Coupling over VIII Group Metals: Elucidation of the Guerbet Reaction Mechanism by DRIFTS. *Ind. Eng. Chem. Res.* **2017**, *56*, 13310–13321. [[CrossRef](#)]
59. Granata, A.; Argyropoulos, D.S. 2-Chloro-4,4,5,5-tetramethyl-1,3,2-dioxaphospholane, a Reagent for the Accurate Determination of the Uncondensed and Condensed Phenolic Moieties in Lignins. *J. Agric. Food Chem.* **1995**, *43*, 1538–1544. [[CrossRef](#)]